

Palmitoylation of Amyloid Precursor Protein Regulates Amyloidogenic Processing in Lipid Rafts

Raja Bhattacharyya, Cory Barren, and Dora M. Kovacs

Neurobiology of Disease Laboratory, Genetics and Aging Research Unit, Department of Neurology, MassGeneral Institute for Neurodegenerative Diseases, Massachusetts General Hospital, Harvard Medical School, Charlestown, Massachusetts 02129

Brains of patients affected by Alzheimer's disease (AD) contain large deposits of aggregated amyloid β -protein ($A\beta$). Only a small fraction of the amyloid precursor protein (APP) gives rise to $A\beta$. Here, we report that $\sim 10\%$ of APP undergoes a post-translational lipid modification called palmitoylation. We identified the palmitoylation sites in APP at Cys¹⁸⁶ and Cys¹⁸⁷. Surprisingly, point mutations introduced into these cysteines caused nearly complete ER retention of APP. Thus, either APP palmitoylation or disulfide bridges involving these Cys residues appear to be required for ER exit of APP. In later compartments, palmitoylated APP (*palAPP*) was specifically enriched in lipid rafts. *In vitro* BACE1 cleavage assays using cell or mouse brain lipid rafts showed that APP palmitoylation enhanced BACE1-mediated processing of APP. Interestingly, we detected an age-dependent increase in endogenous mouse brain *palAPP* levels. Overexpression of selected DHHC palmitoyl acyltransferases increased palmitoylation of APP and doubled $A\beta$ production, while two palmitoylation inhibitors reduced *palAPP* levels and APP processing. We have found previously that acyl-coenzyme A:cholesterol acyltransferase (ACAT) inhibition led to impaired APP processing. Here we demonstrate that pharmacological inhibition or genetic inactivation of ACAT decrease lipid raft *palAPP* levels by up to 76%, likely resulting in impaired APP processing. Together, our results indicate that APP palmitoylation enhances amyloidogenic processing by targeting APP to lipid rafts and enhancing its BACE1-mediated cleavage. Thus, inhibition of *palAPP* formation by ACAT or specific palmitoylation inhibitors would appear to be a valid strategy for prevention and/or treatment of AD.

Introduction

Deposition of the amyloid ($A\beta$) peptide in senile plaques is a hallmark of Alzheimer's disease (AD) pathology (for review, see Tanzi et al., 2004; Walsh and Selkoe, 2004; Haass and Selkoe, 2007). $A\beta$ derives from the amyloid precursor protein APP, which is a type 1 transmembrane protein. APP undergoes sequential proteolysis by three types of proteases, α -, β - and γ -secretases. Proteolysis of APP by α - and γ -secretases releases soluble nonamyloidogenic p3 peptides, while β - and γ -secretase cleavages generate amyloidogenic $A\beta$ peptides of various length ranging from 30 to 42 aa (Kojro and Fahrenholz, 2005; Steiner et

al., 2008). $A\beta_{42}$ peptides in particular form the most pathogenic oligomers and aggregates (Iwatsubo et al., 1994).

Although the proteolytic events resulting in $A\beta$ production are well characterized, it is not clear why only a small portion of APP undergoes amyloidogenic processing (Haass et al., 2012). Shortly after synthesis in the ER, APP traffics to the Golgi and eventually to the plasma membrane. Approximately 10% of total APP is cleaved by α -secretase at the plasma membrane to generate a soluble ectodomain APP (sAPP), sAPP α , and a truncated C-terminal fragment (α -CTF), while the majority of the plasma membrane bound APP is rapidly endocytosed (Kojro and Fahrenholz, 2005; Thinakaran and Koo, 2008). Alternatively, APP can be processed by BACE1 to generate sAPP β and β -CTF in the trans-Golgi, plasma membrane, and early endosomes (Selkoe, 1998; De Strooper and Annaert, 2000). The β -CTF is further cleaved in the endocytic recycling compartment or late endosomes by the γ -secretase complex to release $A\beta$ (Haass et al., 1992). Interestingly, APP, BACE1 and γ -secretase components are all found in membrane microdomains known as detergent-resistant lipid rafts (Vetrivel et al., 2004, 2005; Hattori et al., 2006).

Protein palmitoylation consists of a thioester linkage between a 16 carbon palmitic acid and a cysteine residue, often resulting in lipid raft localization of the protein (Resh, 2004; Brown, 2006). The primary function of protein palmitoylation is to enhance hydrophobicity of proteins and thereby facilitate association with membrane components of the cell and hydrophobic domains of other proteins (Charollais and Van Der Goot, 2009). The proper

Received Oct. 4, 2012; revised April 23, 2013; accepted May 27, 2013.

Author contributions: R.B. and D.M.K. designed research; R.B. and C.B. performed research; R.B., C.B., and D.M.K. analyzed data; R.B. and D.M.K. wrote the paper.

This work was supported by Cure Alzheimer's Fund grants and NIH–NINDS Grant R01NS45860 (D.M.K.). We thank Dr. Vivek Gautam (Massachusetts General Hospital, Charlestown, MA) for his generous help in preparing primary neurons; Dr. Masaki Fukata (National Institute for Physiological Sciences, Okazaki, Japan) for providing us with the DHHC expression plasmids; Dr. Kiyohito Mizutani (Kobe University Graduate School of Medicine, Kobe, Japan; previously at Massachusetts General Hospital, Charlestown, MA) for generating APP(Δ 343)-expressing cells; Dr. Jordan Tang (Oklahoma Medical Research Foundation, Oklahoma City, OK) for dr9; Lit-Fui Lau (GlaxoSmithKline, Shanghai, China; previously at Pfizer, Groton, CT) for CI-1011; and Dr. Doo Yeon Kim (Massachusetts General Hospital, Charlestown, MA) for helpful advice and discussions.

The authors declare no competing financial interests.

Correspondence should be addressed to Dora M. Kovacs, Neurology of Disease Laboratory, Genetics and Aging Research Unit, Department of Neurology, MassGeneral Institute for Neurodegenerative Diseases, Massachusetts General Hospital, Harvard Medical School, Charlestown, MA 02129. E-mail: dora_kovacs@hms.harvard.edu.

DOI:10.1523/JNEUROSCI.4704-12.2013

Copyright © 2013 the authors 0270-6474/13/3311169-15\$15.00/0

activity of oncoproteins such as H-ras is dependent on their state of palmitoylation resulting in lipid raft localization (Rocks et al., 2005). In the brain, protein palmitoylation is the most abundant lipid modification among neuronal proteins (Fukata and Fukata, 2010). BACE1 and two components of γ -secretase, Aph-1 and nicastrin (Nct), are targeted to lipid rafts by post-translational palmitoylation of C-terminal cysteine residue(s) near their transmembrane domains (Cheng et al., 2009; Vetrivel et al., 2009). Although palmitoylation-deficient mutants of BACE1, Aph-1, and Nct do not exhibit altered APP processing *in vitro* (Cheng et al., 2009; Vetrivel et al., 2009), lack of Aph-1 or Nct palmitoylation may affect γ -secretase activity *in vivo* (Meckler et al., 2010).

Here, we report for the first time that APP undergoes palmitoylation in its N-terminal E1 luminal domain. Mutations introduced into APP's palmitoylated cysteines result in ER retention of the protein. Palmitoylated APP is preferentially targeted to lipid raft domains where it serves as a good BACE1 substrate in cells and *in vivo*. Palmitoylation inhibitors severely impair the processing of APP by α - and β -secretases. Acyl-coenzyme A:cholesterol acyltransferase (ACAT) inhibitors, which redistribute cellular cholesterol, also inhibit APP palmitoylation and reduce A β generation. Thus, APP palmitoylation appears to promote lipid raft-bound A β production.

Materials and Methods

Cell culture and transfection

CHO_{APP}, H4, and naive CHO cells were maintained and transfected with expression plasmids as described previously (Huttunen et al., 2007b, 2009). CHO cells stably expressing APP and myc-epitope-tagged BACE1 (CHO_{APP+BACE1}) were maintained in DMEM containing 10% serum supplemented with G418 and Zeocine. AC29_{APP} cells that lack ACAT activity were grown as described previously (Puglielli et al., 2001). Typically, 1.2×10^6 cells were used for transfection and palmitoylation assays.

Preparation of hippocampal primary neurons

Primary neuronal cultures were prepared as described previously (Puglielli et al., 2001). Briefly, hippocampi and frontal cortices of CD-1 mice (Charles River Laboratories International) were dissected from embryonic day 16 (E16)–E18. The tissues were triturated and plated for overnight on poly-(L-lysine)-coated (0.2 mg/ml) culture dishes at the concentration of 32,000 cells/cm². Neurons were then maintained in Neurobasal medium with 2% B27 supplement (Invitrogen) at 37°C with 5% CO₂ in air for 14 d. Postculture primary neurons were used for BACE1-inhibition and palmitoylation assays.

Expression plasmids and antibodies

C-terminally V5-epitope-tagged APP₇₅₁ (APP_{wt-V5}) were used as described previously (Huttunen et al., 2007b). N-terminal truncation mutants APP(Δ 281) and APP(Δ 343) were subcloned into pCDNA3.1-V5/His vector. cDNA of APP_{wt-V5} was used to prepare the cysteine mutants APP(C^{186,187}S/A), APP(C¹⁸⁶S), APP(C¹⁸⁷S), C^{186/187}E/Q/R/F/P, and APP(C^{133/158}S/A) by using appropriate mutagenesis primer pairs and the QuikChange site-directed mutagenesis kit (Invitrogen). cDNAs encoding HA-epitope-tagged DHHC (Asp-His-His-Cys)-1, DHHC-7, and DHHC-21 (HA-DHHC-1, HA-DHHC-7, and HA-DHHC-21, respectively) were kind gifts from Dr. M. Fukata (National Institute for Physiological Sciences, Okazaki, Japan; Fukata et al., 2004). The following APP antibodies were used: C66 (APP C-terminus), 22C11 (APP N-terminus; Millipore Bioscience Research Reagents), anti-sAPP β (IBL International), and 6E10 (Signal). Polyclonal antibody against BACE was obtained from Affinity BioReagents. Antibodies against epitope tags were anti-V5 (Invitrogen), anti-myc and anti-HA (Cell Signaling Technology). Antibodies against calreticulin (ER marker), GM130 (Golgi marker), and flotillin (lipid rafts marker) were obtained from Santa Cruz Biotechnology, BD Biosciences, and Abcam, respectively.

Western blot analysis

Cell lysates were prepared by directly extracting cells in a buffer containing 10 mM Tris-HCl at pH 6.8, 1 mM EDTA, 150 mM NaCl, 0.25% NP-40, 1% Triton X-100, and a protease inhibitor cocktail (Roche), followed by centrifugation at 16,000 \times g. For modified acyl-biotinylation exchange assay (mABE assay), the lysis buffer was complemented with 10 mM tris(2-carboxyethyl)phosphine (TCEP; Sigma) and 10 mM N-ethylmaleimide (NEM; Thermo Scientific). Proteins (20–100 μ g) were subjected to immunoprecipitation or ABE assay, or simply resolved on 4–12% gradient Bis-Tris gels, 12% Bis-Tris gels, or 16% Tricine gels (Invitrogen), depending on the individual experiment, as described. The blots were visualized by enhanced chemiluminescence. The images were captured by using BioMax film (Kodak) and quantified using QuantityOne software (Bio-Rad).

Preparation of mouse brain lysates

All experimental procedures were performed in accordance with the U.S. Public Health Service *Guide for Care and Use of Laboratory Animals* and were approved by the Massachusetts General Hospital Subcommittee on Research Animal Care. Mice used in the study were of either sex. BACE1-null and wild-type (WT) control mice (C57BL/6J background) were purchased from The Jackson Laboratory. BACE1-heterozygous knock-out mice (BACE1^{-/-}) were generated by crossing BACE1-null and wild-type control mice as described previously (Kim et al., 2011). Three-month-old mice were killed, and brains were immediately removed and stored at -80°C until use. Cortices were obtained immediately after the brains were removed and immediately stored at -80°C until use. Membrane extracts from total brains or cortices were prepared as described previously (Kim et al., 2011). For ABE assays, extracts were prepared according to the published method (Wan et al., 2007). To assess changes in palmitoylated APP (*palAPP*) levels in cortices from young versus older mice, three 3-month-old and three 18-month-old nontransgenic (non-Tg) mice (C57BL/6J background; The Jackson Laboratory) were used. Mouse brain lysates were prepared as above.

Lipid raft and subcellular fractionations

Lipid rafts were isolated from 0.5% Lubrol WX (Lubrol 17A17; Serva) lysates of cultured cells by discontinuous flotation density gradients as described previously (Vetrivel et al., 2009). For the isolation of lipid rafts from mouse brain, we essentially followed published methods (Vetrivel et al., 2005). Briefly, mouse brains were homogenized in five volumes of HBS (50 mM HEPES pH 7.4, 0.15 M NaCl, 5 mM EDTA) before addition of 0.5% Lubrol. The extracts were sonicated three times for 30 s using a microsonicator and centrifuged at 2500 \times g for 10 min to remove cell debris and nuclei. The supernatant were adjusted to 40% sucrose and separated on a discontinuous sucrose density gradient. Subcellular organelles were separated by subjecting cell lysates to OptiPrep fractionation analysis as done previously (Huttunen et al., 2009).

Palmitoylation assays

Metabolic labeling with [³H] palmitic acid. CHO-APP cells were metabolically labeled with [³H] palmitic acid ([³H]-C16; PerkinElmer) as described previously (Vetrivel et al., 2009). Briefly, cells were incubated with 10 mCi [³H]-C16 for 6 h before lysis in 10 mM Tris-HCl, pH 7.6, 2 mM EDTA, and 150 mM NaCl containing protease inhibitors. APP were immunoprecipitated from the labeled cells by anti-APP (C-terminus) antibody C66. The immunoprecipitates were subjected to fluorography as done previously (Bhattacharyya and Wedegaertner, 2000).

Metabolic labeling with Alkyl-C16. Briefly, cells were metabolically labeled with a chemical palmitic acid probe, alkylene palmitic acid (Alkyl-C16; Invitrogen) as described previously (Charron et al., 2009). Six hours after labeling, cells were subjected to immunofluorescence analysis as described previously (Charron et al., 2009). For Western blots, cells were lysed, and APP was immunoprecipitated from the lysates on agarose beads before reacting with a bioorthogonal alkyne-labeled fluorescent chromophore, tetramethylrhodamine (alkyne-TAMRA; Invitrogen) via “click chemistry” (Charron et al., 2009). The samples were then probed with an anti-TAMRA antibody (Invitrogen).

ABE assay. This assay is based on the substitution of biotin for palmitoyl modifications through a sequence of three chemical steps: unmodified cysteine thiols are blocked with NEM; palmitoylation thioesters are

cleaved by hydroxylamine (+NH₂OH); and finally, the newly exposed cysteinyl thiols are marked with thiol-specific biotinylating reagent (HPDP-biotin in our experiments). Biotinylated proteins are then affinity purified with streptavidin–agarose beads and probed for the protein of interest (Komekado et al., 2007; Kang et al., 2008). Briefly, cells were lysed with lysis buffer (50 mM Tris-HCl, pH 7.5, 150 mM NaCl, 5 mM EDTA) containing 1% SDS, 2% Triton X-100, 0.5% NP-40, protease inhibitors, 10 mM TCEP (Sigma), and 10 mM NEM (Thermo Scientific). Equal amounts of proteins were precipitated by chloroform-methanol before 1 M NH₂OH treatment (untreated samples served as controls), HPDP-biotin addition, and affinity purification with StreptAvidin agarose. The precipitates were either probed with an appropriate antibody or Streptavidin-HRP to detect palmitoylated proteins. In some cases, cells were treated with palmitoylation inhibitors 2-bromopalmitate (2-BP) and cerulenin (Sigma) before ABE assay. In addition, while testing the effect of ACAT inhibition on APP palmitoylation, cells were treated with ACAT inhibitors CP-113,818 (CP) or CI-1011 [avasimibe (AV)], as described previously (Huttunen et al., 2007a, 2010) before ABE assay. CP and AV were generous gifts from Dr. J. Harwood (Pfizer, Groton, CT) and L.-F. Lau (GlaxoSmithKline, Shanghai, China), respectively. For lipid raft and nonraft palmitoylation studies, protein extracts from lipid rafts and nonrafts were subjected to ABE assay according to a method reported previously (Yang et al., 2010). Briefly, lipid raft fractions were extracted with 60 mM β -octyl glucoside (Sigma), and nonraft fractions were extracted with 1% Triton X-100. The protein extracts were precipitated using chloroform/methanol before ABE assay.

Modified ABE assay. This assay is based on a modification of the ABE assay as described previously (Cheng et al., 2009). Briefly, cells were lysed in lysis buffer (150 mM NaCl, 5 mM EDTA, 50 mM Tris-HCl, pH 7.4, 1% Triton X-100, protease inhibitors, 10 mM TCEP, and 10 mM NEM). Aliquots of lysates were incubated with appropriate antibodies to immunoprecipitate APP or sAPP. Immunoprecipitated proteins bound to agarose beads were treated with 1 M NH₂OH, pH 7.4, followed by incubation with biotin-HPDP at 4°C for 2 h to label the reactive cysteine(s). A sample prepared in absence of NH₂OH served as negative control. The beads were washed and immunoblotted with streptavidin-HRP (Cell Signaling Technology) to detect palmitoylation.

Fluorescence imaging of palmitoylated proteins

CHO cells expressing APP-V5 were grown on coverslips and metabolically labeled Alkyl-C16 (100 μ M in DMSO) or DMSO. Six hours after labeling, cells were subjected to “click-it” assay using alkyne-TAMRA as described previously (Charron et al., 2009). After TAMRA labeling, cells were stained with anti-V5 antibody (Santa Cruz Biotechnology) to detect distribution of APP-V5 (Huttunen et al., 2007b). Confocal images were obtained using an Olympus DSU/IX70 spinning disc confocal microscope equipped with IPLab software (Scanalytics/BD Biosciences) for image processing.

A β ₄₀ and A β ₄₂ determinations

For A β determination, cells stably transfected with wild-type or mutant APP₇₅₁ were grown in six-well plates (Becton Dickinson Labware). When ~80–90% confluent, cells were washed in PBS and incubated in 1 ml of fresh medium for 24 h. Secreted A β ₄₀ and A β ₄₂ were quantified by standard sandwich ELISA using the commercially available A β ELISA kit (Wako Pure Chemical). Values were normalized by the total cellular protein amount. For the experiments with HA-DHHC-1, HA-DHHC-7 and HA-DHHC-21, CHO_{APP} cells were transiently transfected with the expression plasmids in six-well plates. Twenty-four hours post-transfected cells were washed with PBS and incubated in 1 ml fresh media for 24 h before A β ELISA assay.

Cyclohexamide block and release assay

CHO_{APP} cells were pretreated with increasing amounts of the BACE inhibitor IV (BACEi IV; 0–5 μ M) for 12 h in presence of 10 μ g/ml cyclohexamide (CHX; Calbiochem) for the last 6 h to block protein synthesis. Cells were incubated for another 4 h in absence of CHX but in presence of the BACE inhibitor before ABE assay to detect newly synthesized *pal*APP.

In vitro BACE-cleavage assay of *pal*APP

BACE-cleavage assays in lipid raft fractions were performed by combining methods reported previously by Wada et al. (2003) and Yamakawa et al. (2010). Briefly, lipid rafts were isolated from the NEM-supplemented Lubrol extract of cells or mouse brains. The lipid raft fractions were pooled and used as a source for *pal*APP for the β -cleavage assay. The substrate was mixed with a 50 mM Na-acetate buffer at pH 4 containing a complete protease inhibitor mixture (Roche Applied Science), the aspartic protease inhibitor pepstatin A (10 μ M; Roche Applied Science), and the γ -secretase inhibitor *N*-[*N*-(3,5-difluorophenacetyl-L-alanyl)]-L-(S)-phenylglycine *t*-butyl ester (0.5 μ M; Calbiochem). BACE activity was measured by incubating the mixture at 37°C in absence or presence of increasing concentration of the β -secretase inhibitors BACEi IV (Calbiochem) or dr9 (a kind gift from Dr. J. Tang, Oklahoma Medical Research Foundation, Oklahoma City, OK; Kim et al., 2007). After 1 h incubation, the reaction was terminated by increasing the pH to 7.6. The mixtures were reacted with 10 mM NH₂OH to detach palmitate from the released sAPP β . The samples were centrifuged at 100,000 \times g for 1 h to remove membranes, and the supernatant were subjected to immunoprecipitation with anti-sAPP antibody 22C11. The mABE assays were performed on the precipitated samples using biotin-HPDP to label the exposed reactive cysteine(s). The beads were washed after biotinylation and probed with streptavidin-HRP or anti-sAPP β antibody to detect palmitoylated sAPP β (*pal*-sAPP β) or sAPP β , respectively.

Statistical analysis

All statistical analyses used a two-tailed Student's *t* test or one-way ANOVA, followed by a *post hoc* Tukey's test. Error bars represented in graphs denote the SEM. Significance was assessed at *p* < 0.05 and *p* < 0.01.

Results

APP is palmitoylated

To test whether APP undergoes palmitoylation, we used CHO cells stably expressing wild-type APP₇₅₁ (CHO_{APP}) in three different palmitoylation assays: metabolic labeling with the fluorescent reactive palmitic acid analog alkylene-palmitic acid (Alkyl-C16), metabolic labeling with [³H]palmitic acid ([³H]-C16), and ABE assay (Fig. 1). To visualize Alkyl-C16 incorporation, we metabolically labeled CHO cells expressing V5-epitope tagged APP (CHO_{APP}) with Alkyl-C16 and performed fluorescent microscopy analysis of cells after incorporation of fluorescently labeled alkyne-TAMRA by “click chemistry” (Charron et al., 2009). We observed colocalization of APP with TAMRA in Golgi-like puncta, indicating that proteins labeled with the palmitic acid probe Alkyl-C16 colocalized with APP at this site (Fig. 1A). To show incorporation of Alkyl-C16 into APP, CHO_{APP} cells were first metabolically labeled with (Alkyl-C16) followed by immunoprecipitation of APP using the anti-APP C-terminal antibody C66. The immunoprecipitates were then subjected to click chemistry using alkyne-TAMRA that interacted with Alkyl-C16. An anti-TAMRA antibody detected Alkyl-C16 labeling of APP (Fig. 1B, left). The palmitoylation inhibitor 2-BP reduced APP palmitoylation to a large extent (Fig. 1B, left). Staining for APP confirmed the presence of equal amounts of APP among the three immunoprecipitated samples (Fig. 1B, right). Direct incubation of CHO_{APP} cells with [³H]palmitic acid ([³H]-C16) followed by immunoprecipitation with the APP antibody C66 showed a single labeled band at ~100 kDa that was absent in samples precipitated with the preimmune serum (Fig. 1C). This band, visible after 2 months of exposure, corresponds to immature APP. Mature ([³H]-C16-labeled) *pal*APP, less abundant than immature *pal*APP (Fig. 1B, D–F), was not visible after 2 months of exposure of the film. These experiments indicate that APP is palmitoylated.

Next we used an ABE assay to explore whether APP undergoes S-palmitoylation as opposed to N-palmitoylation (Roth et al.,

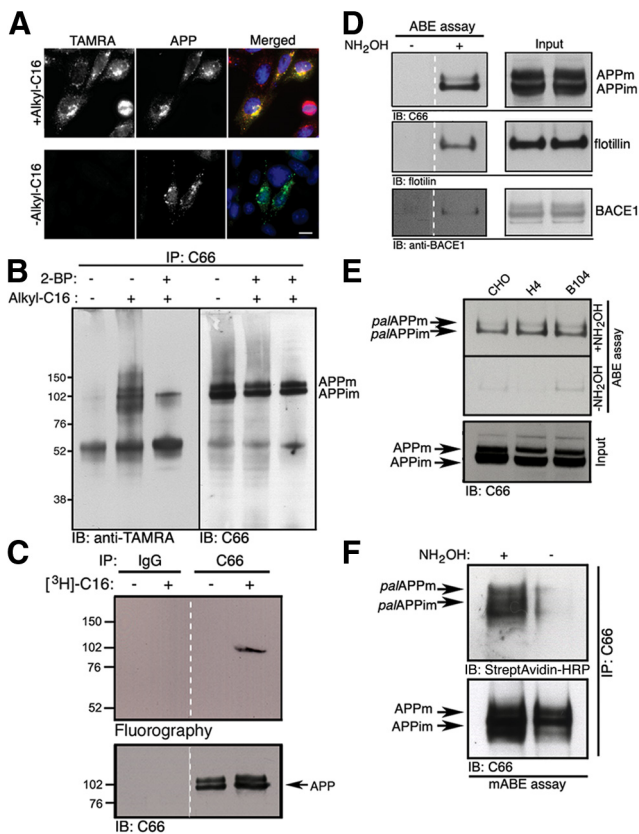


Figure 1. APP is palmitoylated. **A**, Confocal microscopy of palmitoylated proteins in CHO_{APP} cells after metabolic labeling with (+) or without (–) Alkyl-C16 followed by alkyne-TAMRA incorporation. APP distribution is detected by immunostaining with anti-V5 antibody (APP). Merged images show colocalization. Scale bar, 10 μ m. **B**, Palmitoylated APP from CHO_{APP} cells metabolically labeled with Alkyl-C16 (left). The palmitoylation inhibitor 2-bromopalmitate (Alkyl-C16 plus 2-BP) prevented incorporation of Alkyl-C16 into APP. APPm, Mature APP; APPim, immature APP. **C**, Top, Fluorography of palmitoylated APP after metabolic labeling of CHO_{APP} cells with 100 μ M [³H]-palmitic acid ([³H]-C16) and immunoprecipitation with an anti-APP C-terminal antibody (C66). Bottom, Total input of APP. **D**, Left, ABE assay showing palAPP, pal-flotillin, and pal-BACE1, not found in the negative control lacking (–) NH₂OH (left). Right, Total input. **E**, ABE assay detected mature and immature palAPP in naive CHO, H4, and B104 cells (top). **F**, Top, Detection of mature and immature palAPP in 3-month-old mouse brain extracts by mABE assay. Bottom, Total immunoprecipitated APP.

2006). The assay consists of replacing thioester-linked palmitates attached to cysteine residues with a thiol-specific biotinylating reagent in the presence of NH₂OH (Komekado et al., 2007; Kang et al., 2008). Palmitoylated proteins are isolated by affinity purification using NeutrAvidin beads. Both immature and mature APP showed NH₂OH-dependent palmitoylation in CHO_{APP} cells, indicating S-palmitoylation of APP (Fig. 1D). Endogenous flotillin, a known palmitoylated protein, also showed NH₂OH-dependent palmitoylation in our cell line (Fig. 1D). Despite weak expression of endogenous BACE1 in CHO cells, we were able to detect endogenous palmitoylated BACE1 in the NH₂OH-treated sample (Fig. 1D) (Vetrivel et al., 2009). Quantitation of the ABE assay results revealed that 10.6 \pm 1.5% of total APP undergoes palmitoylation in CHO_{APP} cells.

Finally, we asked whether endogenous APP undergoes palmitoylation in naive cell lines and mouse brain extracts. Our ABE assay detected both immature and mature palAPP in naive CHO cells, H4 human neuroglioma cells, and B104 rat neuroblastoma cells (Fig. 1E). Quantitative analysis revealed palmitoylation of ~7% endogenous APP in naive CHO cells. Strikingly, we could

also identify both endogenous immature and mature palAPP by mABE using non transgenic mouse brain extracts (Fig. 1F). Together, all three different methods used showed for the first time that APP is palmitoylated.

APP is palmitoylated at Cys¹⁸⁶ and Cys¹⁸⁷

Next, we asked which protein domain of APP harbors the palmitoylated cysteine residues. Given that APP lacks cysteine residues in its cytosolic domain, we used N-terminal deletion mutants of the protein. We performed ABE assays on the neuronal APP isoform APP₆₉₅, which lacks the KPI domain containing 6 cysteine residues, on APP(Δ 281) that lacks 12 N-terminal cysteine residues, and on APP(Δ 343) lacking both the KPI and the cysteine-rich domains (Fig. 2A). Our results showed that APP₆₉₅ was palmitoylated similarly to APP₇₅₁ (~98%), indicating that one or more of the 12 cysteine residues in the N-terminal region between Cys³⁸ and Cys¹⁸⁷ are palmitoylated (Fig. 2B,C). Indeed, APP(Δ 281) showed little or no palmitoylation (~9%), confirming that the six cysteine residues in the KPI domain play a minimal role in APP₇₅₁ palmitoylation (Fig. 2B,C). APP(Δ 343) resulted in complete loss of palmitoylation, as expected given the absence of cysteines in this protein (Fig. 2B,C). Therefore, effective palmitoylation of APP occurs in its N-terminal domain between Cys³⁸ and Cys¹⁸⁷. These data confirm that APP undergoes luminal palmitoylation, similarly to Sonic Hedgehog, Spitz, or Wnt (Resh, 2006; Buglino and Resh, 2008).

A precise consensus sequence for protein palmitoylation is not known. However, a previously developed palmitoylation site prediction algorithm with a clustering and sorting strategy allows for identification of potential palmitoylation sites with >80% sensitivity and specificity (Zhou et al., 2006). Applying this strategy, we identified two cysteine residues at positions 186 and 187 as potential candidates for S-palmitoylation. This prediction was confirmed in our systematic mutation analysis, where we independently mutated all 12 cysteine residues between Cys³⁸ and Cys¹⁸⁷ and performed palmitoylation assays (data not shown). The top panel of Figure 2D shows that site-directed mutagenesis of cysteine residues 186 and/or 187 to serines or alanines prevented palmitoylation of APP.

Next, we characterized APP Cys¹⁸⁶ and/or Cys¹⁸⁷ for changes in trafficking and processing. Stably transfected CHO cells expressing APP(C¹⁸⁶S), APP(C¹⁸⁷S), APP(C^{186,187}S), or APP(C^{186,187}A) generated little or no detectable APP CTFs (Fig. 2D, bottom). APP maturation was also reduced by ~95%, indicating potential ER retention of the mutant proteins (Fig. 2D, bottom). To test for ER retention, we performed a subcellular distribution assay using OptiPrep fractionation. CHO cells stably expressing wild-type APP or the cysteine mutant APP(C^{186,187}S) were subjected to fractionation in 7.5–30% OptiPrep gradients (Fig. 2E). As expected, the localization of wild-type APP showed a gentle shift from the immature protein in the ER (calreticulin) to the mature protein appearing in the Golgi fractions (GM130). In contrast, predominantly immature APP(C^{186,187}S) partitioned exclusively in the calreticulin-positive ER fractions, confirming that APP(C^{186,187}S) is indeed retained in the ER (Fig. 2E). To complement the fractionation analysis, cells expressing wild-type or mutant APP were subjected to indirect immunofluorescence analysis. Confocal microscopy showed typical Golgi-like punctate staining of wild-type APP (Fig. 2F, a–c). In contrast, APP(C^{186,187}S) showed predominant localization to ER-like reticular structures stained with the ER marker calreticulin (Fig. 2F, d–f). Additionally, wild-type APP partially colocalized with the

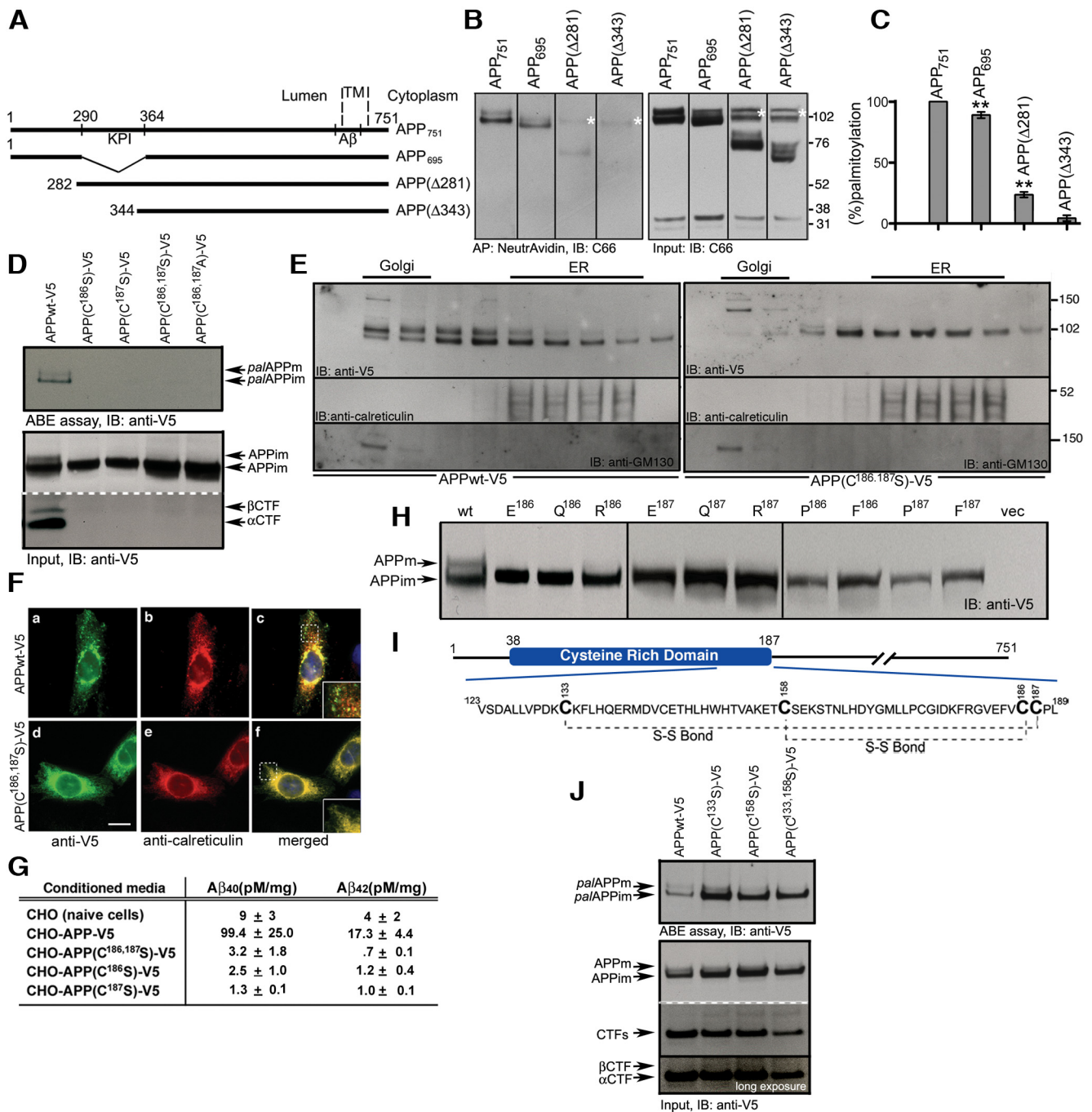


Figure 2. Cys¹⁸⁶ and Cys¹⁸⁷ are required for effective palmitoylation and ER exit of APP. **A**, Schematic representation of APP splice variants, APP₇₅₁ and APP₆₉₅, and N-terminal deletion mutants, APPΔ281 and APPΔ343. **B**, Left, ABE assay showing palmitoylation of APP₇₅₁ and APP₆₉₅, but not of APPΔ281 and APPΔ343. Right, APP protein loads for each assay. Asterisks represent endogenous APP. **C**, Quantitative analysis of **B** and two additional experiments, expressed as percentage of palmitoylation compared to APP₇₅₁. ***p* < 0.01. **D**, Top, APP Cys¹⁸⁶ and/or Cys¹⁸⁷ mutants stably expressed in CHO cells are not palmitoylated in ABE assays. Bottom, Severely reduced maturation and α- and β-CTF generation by the Cys mutants. APP CTFs were overexposed with respect to full-length APP. **E**, OptiPrep density gradient subcellular fractionation shows nearly complete ER retention of the APP(C^{186,187}S) mutant. ER and Golgi fractions were detected by calreticulin and GM130 stainings, respectively. **F**, **a–f**, Indirect immunofluorescence analysis confirms predominant ER (calreticulin positive) localization of the APP(C^{186,187}S) mutant. Scale bar, 10 μm. **G**, Conditioned media from indicated cells were subjected to sandwich ELISA to determine amyloid (Aβ₄₀ and Aβ₄₂) release from the cells. **H**, Additional Cys¹⁸⁶ and/or Cys¹⁸⁷ mutants show lack of APP maturation. **I**, Partial amino acid sequence of APP's cysteine-rich domain, showing the known Cys¹⁸⁶–Cys¹⁵⁸ and Cys¹⁸⁷–Cys¹³³ disulphide bridges (S–S). **J**, Top, APP Cys¹³³ and/or Cys¹⁵⁸ mutants show increased palmitoylation in an ABE assay performed on CHO cells transiently transfected with expression plasmids. Bottom, Maturation and CTF generation of the mutants.

Golgi marker GM130, while APP(C^{186,187}S) did not (data not shown). Not surprisingly, conditioned media from the mutant CHO cells showed >95% decrease in Aβ₄₀ and Aβ₄₂ levels as compared to WT APP-expressing cells (Fig. 2G). Similarly, PC-12 cells transiently expressing APP(C¹⁸⁶S), APP(C¹⁸⁷S), or APP(C^{186,187}S) presented identical results, as all three proteins

generated barely detectable APP CTFs, and their Aβ₄₀ and Aβ₄₂ levels were reduced by 85–95% as compared to transfected WT APP (data not shown). Collectively, these data show that APP is S-palmitoylated at Cys¹⁸⁶ and/or Cys¹⁸⁷ in the ER or early secretory compartments, and that these cysteine residues are required for ER exit of APP.

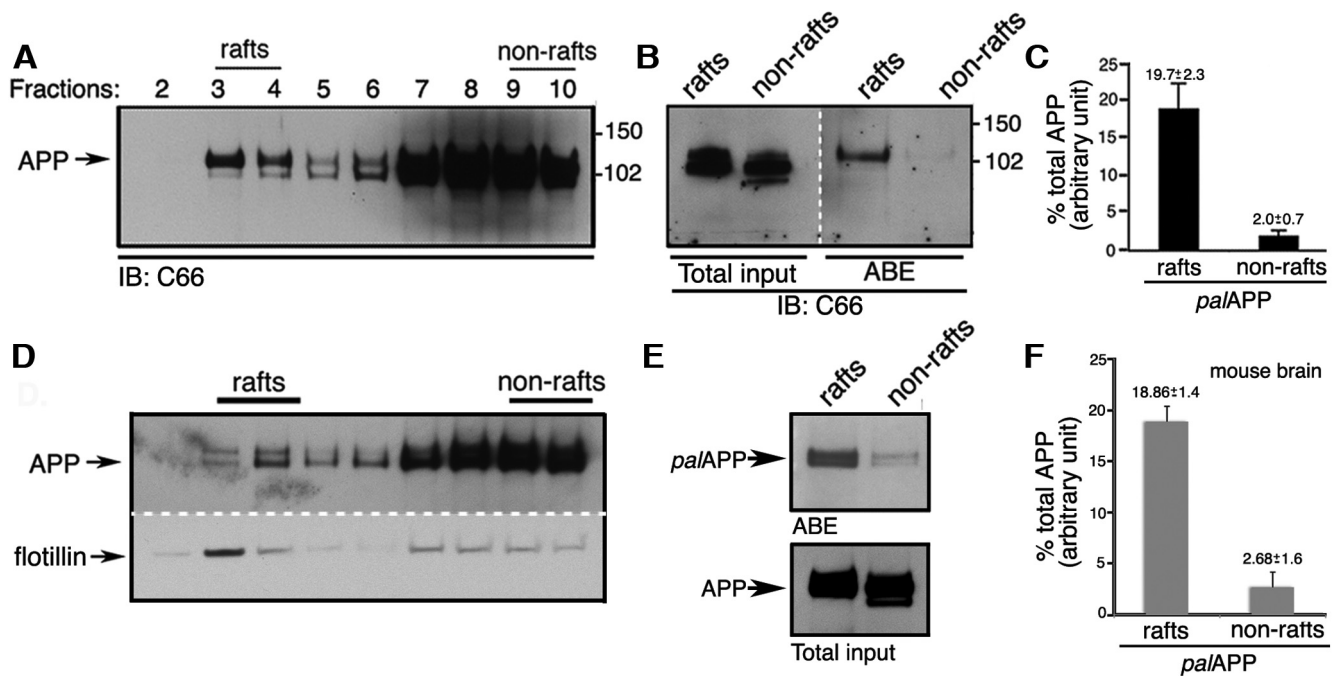


Figure 3. *palAPP* is enriched in lipid rafts. **A**, Lipid raft fractionation of CHO_{APP} cell Lubrol extracts on a discontinuous sucrose gradient. APP is stained with a C-terminal antibody (C66). **B**, ABE assay on raft (3 and 4) and nonraft (9 and 10) fractions normalized for full-length APP amounts (left, Total input), illustrating increased *palAPP* levels in rafts compared to nonrafts (right, ABE). **C**, Quantitation of **B** and two additional experiments, showing *palAPP* in raft fractions compared to non-raft fractions relative to total APP. **D**, Lipid raft fractionation of mouse brain Lubrol extracts. Rafts, Flotillin positive; nonrafts, flotillin negative. **E**, ABE assay on mouse brain raft and nonraft fractions show increased *palAPP* levels in lipid rafts. Representative of triplicate experiments performed on raft and nonraft fractions isolated separately from two non-Tg mice. **F**, Quantitation of **E**. Error bars show the SEM.

We initially reasoned that the nearly complete ER retention of our APP(C^{186,187S}), APP(C^{186,187A}), APP(C^{186S}), or APP(C^{187S}) mutants was due to the serine or alanine residues causing improper folding of the APP ectodomain. To overcome this issue, we created 15 additional APP mutant proteins, each containing a different amino acid replacement of Cys¹⁸⁶ or Cys¹⁸⁷. All 15 mutants generated undetectable or barely detectable levels of mature APP, presumably causing ER retention of each mutant protein (Fig. 2*H*; data not shown). Since only up to 11% of APP is palmitoylated in CHO_{APP} cells, lack of palmitoylation may not account for the dramatic ER retention of Cys¹⁸⁶ or Cys¹⁸⁷ APP mutants. Indeed, Cys¹⁸⁶ and Cys¹⁸⁷ reside within the copper binding domain of APP and are predicted to stabilize domain structure by forming disulfide bonds with Cys¹⁵⁸ and Cys¹³³, respectively (Fig. 2*I*) (Barnham et al., 2003). To confirm that disrupted disulfide bridges contribute to the observed ER retention, we mutated the partner Cys¹⁵⁸ and Cys¹³³ to serines to produce APP(C^{133S}), APP(C^{158S}), and APP(C^{133,158S}) mutants. All three mutants showed enhanced palmitoylation in our ABE assays compared to wild-type APP, apparently due to increased availability of Cys¹⁸⁶ and Cys¹⁸⁷ to incorporate palmitate (Fig. 2*J*, top). This experiment suggests the interesting possibility that disulfide bond formation between Cys¹⁵⁸ and Cys¹⁸⁶ or Cys¹³³ and Cys¹⁸⁷ may regulate APP palmitoylation. Despite a slight increase in palmitoylation, we observed a modest decrease in the maturation of all three mutant APP proteins, confirming that disulfide bridges between Cys¹⁵⁸ and Cys¹⁸⁶ or Cys¹³³ and Cys¹⁸⁷ are also essential for ER exit of the protein (Fig. 2*J*, bottom). Interestingly, we noticed a trend for slightly increased β -CTF levels as compared to wild-type APP in all three mutants (Fig. 2*J*, bottom). Together, our data show that palmitoylation at Cys¹⁸⁶ and Cys¹⁸⁷ or disulfide bonds between Cys¹⁵⁸ and Cys¹⁸⁶ or Cys¹³³ and Cys¹⁸⁷ are important for

ER exit of APP, and suggest for the first time that increased APP palmitoylation may enhance β -cleavage of APP.

palAPP is highly enriched in lipid rafts

Since mutations inserted into Cys¹⁸⁶ or Cys¹⁸⁷ resulted in nearly full ER retention of APP, these mutants could not be used to assess the effect of APP palmitoylation on APP metabolism. To begin assessing the effect of APP palmitoylation on APP trafficking, we first asked whether *palAPP* is enriched in lipid rafts compared to nonrafts. Indeed, a prominent function of palmitoylation is to recruit proteins to cholesterol-rich lipid raft microdomains (Resh, 2004; Brown, 2006). We first isolated lipid raft and non-lipid raft fractions from CHO_{APP} cells using discontinuous sucrose gradient fractionation (Fig. 3*A*). As expected, total full-length APP was more abundant in nonraft versus raft fractions. To assess relative distribution of *palAPP*, we adjusted the protein concentration in our ABE palmitoylation assay to start with approximately equal levels of total APP (Fig. 3*B*, left). Thus, approximately equal amounts of APP from lipid raft and nonraft fractions were subjected to an ABE assay. Interestingly, the ABE assay demonstrated high *palAPP* levels in lipid raft fractions, while *palAPP* remained nearly undetectable in nonraft fractions (Fig. 3*B*, right). Quantitative analysis revealed that while 19.7 ± 2.3% of lipid raft-bound APP was palmitoylated, only 2 ± 0.7% of nonraft APP showed palmitoylation (Fig. 3*C*). Since 2% of nonraft APP is palmitoylated and full-length APP is mainly localized to nonraft fractions, *palAPP* is also abundantly found in nonraft fractions (for non-raft APP levels, see Fig. 3*A*; 2% of this APP is palmitoylated in CHO_{APP} cells).

To show that palmitoylation also targets APP to lipid rafts *in vivo*, we isolated lipid raft and non-lipid raft fractions from non-Tg mouse brains (Fig. 3*D*). Similarly to the experiments

performed in cells, *palAPP* was detected in mouse brain lipid raft and nonraft fractions (Fig. 3E). Quantitation of these direct ABE assays revealed that $18.86 \pm 1.4\%$ of raft-bound APP was palmitoylated, compared to only $2.68 \pm 1.6\%$ of non-raft APP showing palmitoylation (Fig. 3F). Modified ABE assays on nontransgenic mouse brain extracts confirmed these results (data not shown). Together, these *in vivo* and *in vitro* data indicate that one function of APP palmitoylation is to target *palAPP* to lipid raft fractions, thus perhaps promoting A β generation.

DHHC-7 and DHHC-21 palmitoyl acyltransferases palmitoylate APP and increase A β generation

We next asked whether enhanced APP palmitoylation results in elevated A β production in cells. Palmitoylation is a reversible process regulated by palmitoylating enzymes [palmitoyl acyltransferases (PATs)] and depalmitoylating enzymes. Biochemical and genetic studies have identified a number of PATs, which share an ~50 aa cysteine-rich domain with a conserved Asp-His-His-Cys (DHHC) motif (Mitchell et al., 2006). Several DHHC PATs have been reported to increase palmitoylation of BACE1, especially of its immature form (Vetrivel et al., 2009).

We tested the effect of 23 HA-epitope-tagged DHHC PATs (DHHC-1 to DHHC-23) on APP palmitoylation in transiently transfected CHO_{APP} cells. Similarly to BACE1, several DHHC PATs enhanced APP palmitoylation in our ABE assay (data not shown). DHHC-7 and DHHC-21 were among the most consistent enzymes to increase APP palmitoylation, while DHHC-1 consistently did not (Fig. 4A, ABE assay). DHHC-7 or DHHC-21, but not DHHC-1, expression increased generation of both APP α - and β -CTFs (Fig. 4A, IB: C66). Importantly, DHHC-7 or DHHC-21, but not the control DHHC-1, increased secreted A β_{40} and A β_{42} levels in the conditioned media of CHO cells (Fig. 4B). Similarly, in PC-12 cells, overexpression of DHHC-7 or DHHC-21 also increased palmitoylation of endogenous APP (Fig. 4A), APP CTF generation, and A β_{40} and A β_{42} levels by approximately twofold compared to mock transfected cells (Fig. 4B). These data further confirm that APP is S-palmitoylated and indicate that palmitoylation promotes A β generation.

palAPP is a good substrate for BACE1-mediated cleavage

To directly address whether *palAPP* undergoes β - or α -secretase cleavages, we first looked for their palmitoylated cleavage products *pal-sAPP β* or *pal-sAPP α* in the extracellular milieu of CHO_{APP} cells. Indeed, it is impossible to differentiate between A β or p3 peptides generated from *palAPP* or non-*palAPP*, given that palmitoylation of APP occurs N-terminally from its BACE1 cleavage site. Figure 5A shows that both *pal-sAPP β* and *pal-sAPP α* were detectable in the media of CHO_{APP} cells, indicating that both β - and α -secretases constitutively cleave *palAPP*. Interestingly, levels of *pal-sAPP β* were similar to those of *pal-sAPP α* (Fig. 5A, first lane, top). We usually see predominantly high levels of *sAPP α* when the palmitoylated pool of APP is not specifically examined (Fig. 5A, first lane, bottom).

To further investigate BACE1-mediated processing of *palAPP*, we selectively overexpressed or inhibited BACE1 in CHO cells (Fig. 5A). Stable overexpression of myc-epitope tagged BACE1 (CHO_{APP+BACE1}) not only increased the amount of *sAPP β* by 1.90 ± 0.16 -fold ($p < 0.01$) in the media as expected, but also elevated *pal-sAPP β* levels by 2.21 ± 0.31 -fold ($p < 0.01$) in our ABE assay, confirming that *palAPP* is cleaved by BACE1 (Fig. 5B). Interestingly, *pal-sAPP α* levels decreased upon BACE1 overexpression, further indicating that BACE1-mediated cleavage of *palAPP* is favored over α -secretase pro-

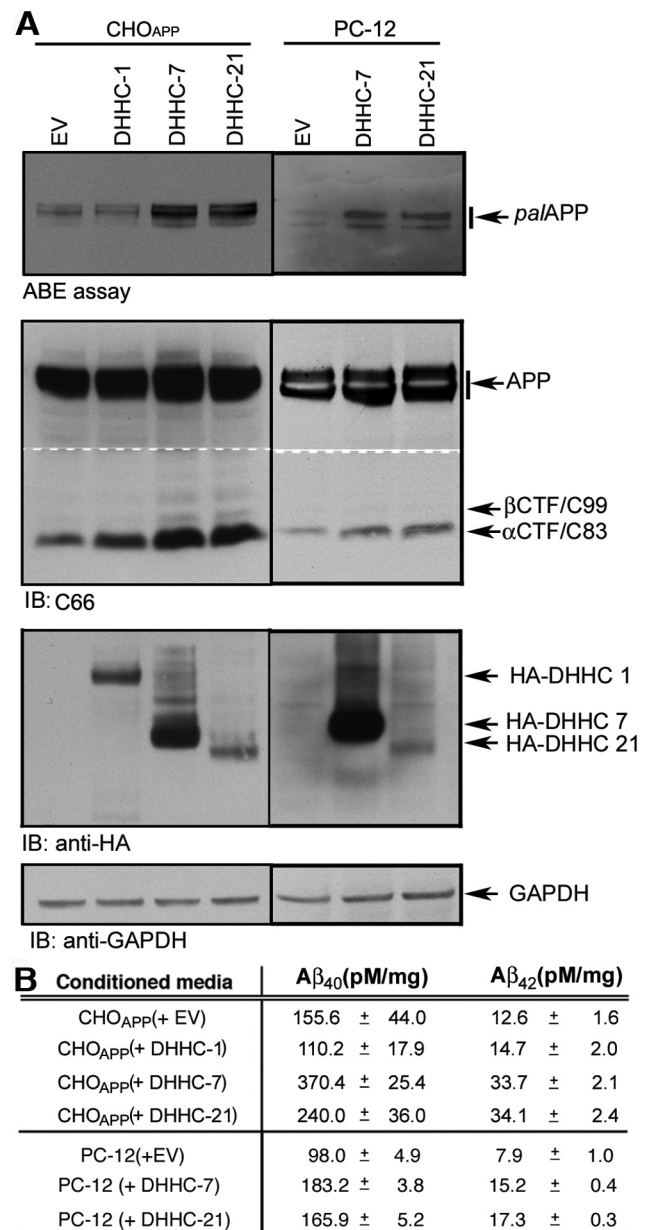


Figure 4. DHHC-7 and DHHC-21 PATs palmitoylate APP. **A**, ABE assay shows increased *palAPP* and α - and β -CTF levels upon expression of HA-DHHC-7 and HA-DHHC-21, but not by expression of HA-DHHC-1 (ABE assay and IB: C66) in CHO_{APP} cells. Similarly, expression of HA-DHHC-7 and HA-DHHC-21 also increased *palAPP* and α - and β -CTF levels in PC-12 cells. Levels of the control GAPDH were unaffected. **B**, A β ELISA demonstrates increased levels of secreted A β_{40} and A β_{42} in the conditioned media isolated from cells (CHO_{APP} and PC-12) expressing HA-DHHC-7 and HA-DHHC-21. HA-DHHC-1 expression shows no effect on A β release from CHO_{APP} cells. Cells transfected with empty vectors (EV) were used as a control.

cessing (Fig. 5A). BACE1 IV reduced *pal-sAPP β* levels in both CHO_{APP} and CHO_{APP+BACE1} cells, again confirming that the released *pal-sAPP β* is indeed a BACE1-cleaved product.

Since BACE1 overexpression increases *pal-sAPP β* levels, levels of its precursor full-length *palAPP* would be expected to concomitantly decrease. To show this, we quantitated total full-length *palAPP* levels in CHO_{APP} as compared to CHO_{APP+BACE1} cells. Indeed, overexpression of BACE1 in CHO_{APP} cells reduced total *palAPP* levels by ~41% (Fig. 5C,D). This was somewhat surprising, as elevated BACE1 activity is known to leave total APP largely unchanged, despite a significant increase in β -CTF/C99

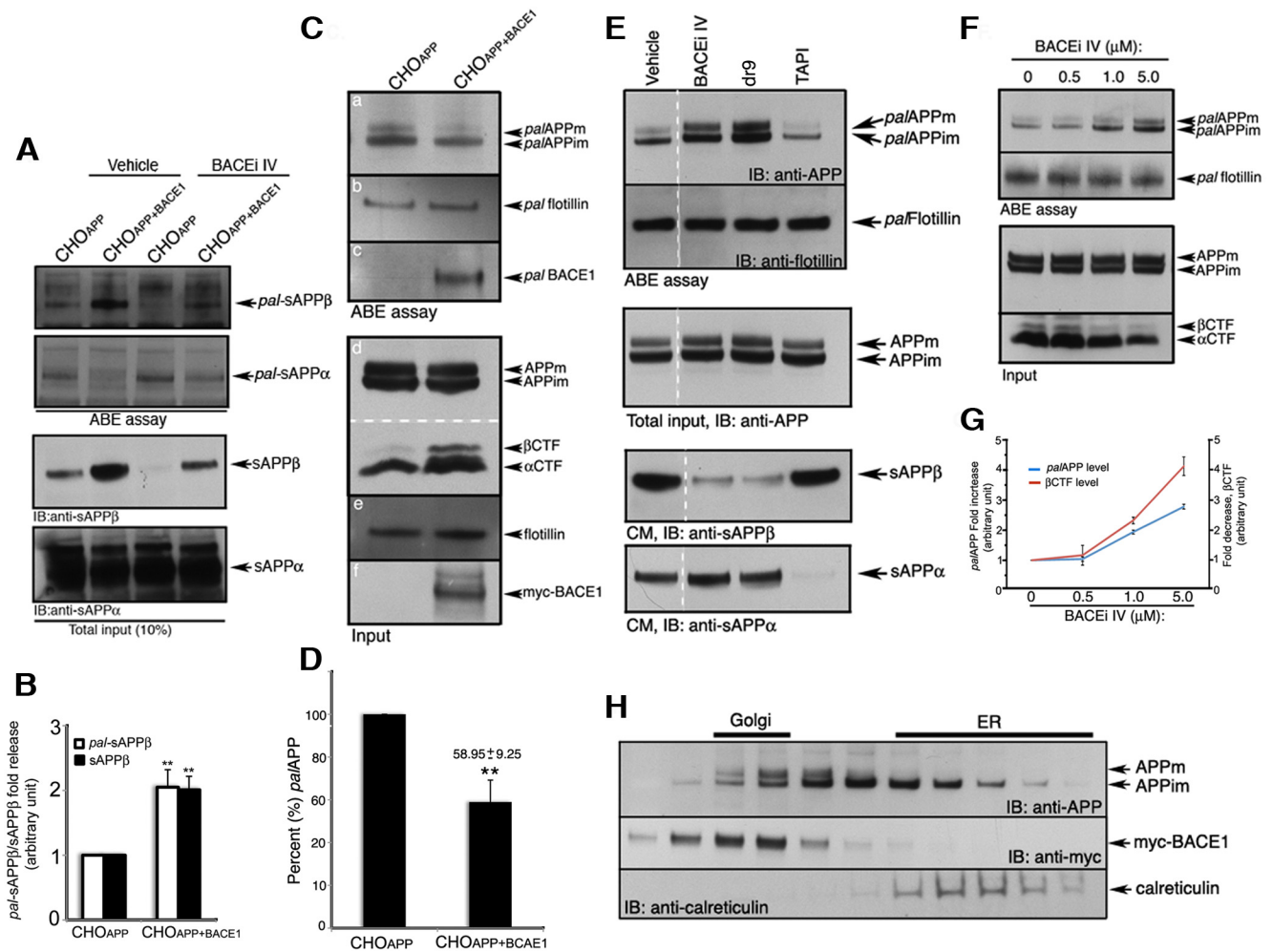


Figure 5. *palAPP* is a better substrate for BACE1 than α -secretase. **A**, Detection of *pal-sAPP β* and *pal-sAPP α* in the conditioned media from CHO_{APP} and CHO_{APP+BACE1} cells (ABE assay). The assay was performed after treating the cells without (Vehicle) or with 5 μ M BACEi IV (BACEi IV) for 16 h. Bottom, Total levels of sAPP β and sAPP α [Total Input (10%)]. ABE assay of the control (Vehicle) conditioned media is the representation of three separate experiments. **B**, Quantitation of the control (Vehicle) ABE assays from **A**. $^{**}p < 0.01$; Error bars indicate SEM. **C**, Top, ABE assay of equal amounts of cell lysates shows reduced full-length *palAPP* in CHO_{APP+BACE1} compared to that from CHO_{APP} (**a**), indicating increased BACE1-mediated cleavage of *palAPP* upon BACE1 expression. Palmitoylated flotillin (**b**) levels remain unchanged in both cells, and palmitoylated BACE1 (**c**) was detected in CHO_{APP+BACE1} cells. Bottom, Total input shows increased β CTF (C99 and perhaps C89) in CHO_{APP+BACE1} cells, but no significant changes in holo-APP (**d**). Total flotillin (**e**) and BACE1 (**f**) are also shown. **D**, Quantitation of **C**. Error bars are the SEM of three separate experiments. **E**, ABE assay of cells treated with 5 μ M BACEi IV, 5 μ M dr9 (dr9), or 20 μ M α -secretase inhibitor (TAPI) demonstrates increased levels of *palAPP* upon BACE inhibition (BACEi IV or dr9), but not α -secretase inhibition (TAPI; top, ABE assay, IB: anti-APP). Pal-flotillin levels remain unchanged (*pal*-flotillin, IB: anti-flotillin). Changes in sAPP β and sAPP α levels show effective BACE and α -secretase inhibition, respectively. **F**, Palmitoylation of newly synthesized APP (*palAPPm* and *palAPPim*) analyzed by CHX block/release assay. APPm, Mature APP; APPim, immature APP. Top, BACEi IV increased newly synthesized full-length *palAPPm* and *palAPPim* in a dose-dependent manner (ABE assay). The bottom panel shows a decrease in β CTF level upon increasing BACEi IV without affecting holo-APP (APPm and APPim) levels. The figure is representative of three separate experiments. **G**, Graphical representation of the *palAPP* fold increase (red) and β CTF fold decrease (blue) of **F**. The error bars are the SEM of three independent experiments. **H**, Postnuclear homogenates of CHO_{APP+BACE1} were fractionated in 7.5–30% OptiPrep density gradients to separate ER and post-ER fractions. Fractions were analyzed for APP (top, APPm and APPim), myc-epitope tagged BACE1 (middle), and the ER-marker calreticulin (bottom).

levels (Fig. 5C, bottom). BACE1 expression did not significantly change palmitoylated flotillin levels (Fig. 5C). These data not only show that *palAPP* undergoes BACE1-mediated cleavage, but also suggest that BACE1 cleaves a larger percentage of *palAPP* than total APP proteins.

After showing that BACE1 overexpression decreases full-length *palAPP* levels, we next asked whether full-length *palAPP* levels increase with BACE or α -secretase inhibition. For these experiments, we used two BACE inhibitors (BACEi IV and dr9) and one α -secretase inhibitor (TAPI) in CHO_{APP} cells. All three inhibitors worked in our experiments, as evidenced by changes in the positive controls sAPP β and sAPP α levels (Fig. 5E, bottom). To detect full-length *palAPP* levels, we used our ABE assay. BACEi IV and dr9, but not the α -secretase inhibitor TAPI, increased the levels of mature and immature *palAPP* (Fig. 5E).

BACEi IV also induced a dose-dependent increase of newly synthesized *palAPP* in cyclohexamide-treated CHO_{APP} cells (Fig. 5F, ABE assay, G). In the same experiment, we detected an inverse correlation between *palAPP* and β -CTF levels (Fig. 5G), while total APP levels remained largely unaffected (Fig. 5F, compare *palAPPm*/*palAPPim*, β CTF). α -CTF levels also decreased to a lesser extent. Subcellular fractionation on an OptiPrep gradient showed that both mature and immature APP colocalize with BACE1 in Golgi compartments, a potential site for BACE1-mediated cleavage of *palAPP* (Fig. 5H). These experiments further confirm that *palAPP* is more efficiently processed by β - than α -secretase in cultured cells.

To test for BACE1-mediated *palAPP* processing under physiological conditions, we asked whether BACE inhibitors would also increase *palAPP* levels in primary neuronal cells. Primary

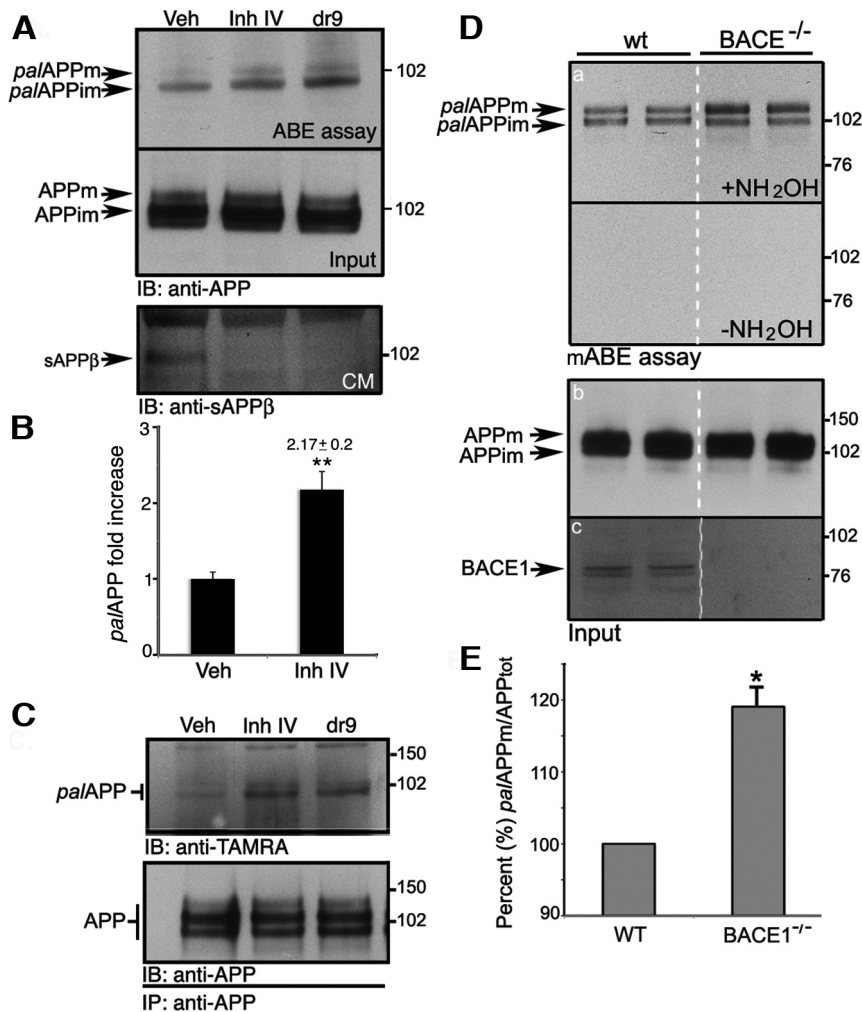


Figure 6. BACE1 cleaves *palAPP* in vivo. **A, C**, Increased full-length *palAPP* levels upon BACE inhibition in primary neurons. Primary neurons generated from nontransgenic mice were incubated with DMSO (veh) or the BACE inhibitors BACEi IV (Inh IV) or dr9 for 16 h before ABE assay (**A**) or metabolic labeling with Alkyl-C16 (**C**). **B**, Quantitation of *palAPP* fold increase upon Inh IV-treatment as in **A**. Error bars represent the SEM of three independent experiments. **C**, TAMRA-labeled *palAPP* was detected by immunoblotting (IB: anti-TAMRA, *palAPP*). **D**, Increased full-length mature *palAPP* levels in cortices of *BACE1*-knock out (*BACE1*^{-/-}) mice compared to control (WT). *palAPP* was measured by performing duplicate mABE assays (**a**) on equal amounts of immunoprecipitated APP (**b**). An anti-BACE1 antibody detected no BACE1 expression in total extract from *BACE1*^{-/-} mice (**c**). **E**, Quantitation of **C**. APP_{TOT} mature APP (APP_m) plus immature APP (APP_{im}). **p* < 0.05; ***p* < 0.01. *n* = 3 for each genotype. Error bar represent the SEM. CM, Conditioned media.

neurons were treated with BACEi IV or dr9 for 16 h. ABE analysis showed elevated *palAPP* levels in BACE inhibitor-treated neurons (Fig. 6A). Treatment with 0.5 μM BACEi IV increased *palAPP* levels by 2.17 ± 0.2-fold compared to vehicle-treated cells (Fig. 6B). As a positive control for effective BACE inhibition in primary neurons, sAPPβ generation was strongly reduced (Fig. 6A, CM). Alkyl-C16 labeling and TAMRA incorporation confirmed these results in a separate experiment (Fig. 6C).

Finally, we asked whether lack of BACE1 expression affects *in vivo palAPP* processing in cortices isolated from age-matched wild-type controls or *BACE1*-knock out (*BACE1*^{-/-}) mice. APP was immunoprecipitated from membrane extracts, and equal amounts of APP were subjected to mABE analysis to detect *palAPP* (Fig. 6D, b). These experiments showed increased levels of mature *palAPP* in *BACE1*^{-/-} compared to wild-type cortices (Fig. 6D, a), further indicating that *palAPP* is a substrate for BACE1 *in vivo*. Interestingly, this ~20% increase was specific for mature *palAPP* (Fig. 6E), while immature *palAPP* and total APP

remained largely unchanged *in vivo* (Fig. 6D, a and b, respectively). Importantly, all our *in vivo* and cell-based data show that *palAPP* is a better substrate for BACE1 than α-secretases. Additionally, the finding that BACE1 cleaves a larger percentage of *palAPP* than total APP proteins indicates that BACE1 may cleave *palAPP* more readily than non-*palAPP*.

Lipid raft-associated *palAPP* is processed by BACE1

Since *palAPP* is efficiently cleaved by BACE1 and is enriched in lipid rafts, we next asked whether BACE1 could cleave *palAPP* in lipid raft fractions. To this end, we performed cell-free *in vitro* BACE-activity assays on lipid raft-associated APP and assayed each reaction for *pal*-sAPPβ levels (Fig. 7). We first separated lipid raft and non-lipid raft fractions from CHO_{APP} cells using a discontinuous sucrose gradient fractionation. Lipid raft fractions were kept at 0°C in a low-pH buffer (pH 4) and warmed to 37°C for BACE1-mediated cleavage of APP and *palAPP*. N-terminal APP fragments were then immunoprecipitated with the anti-APP N-terminal antibody 22C11 and subjected to mABE palmitoylation assay to detect *pal*-sAPPβ. Interestingly, *pal*-sAPPβ levels dramatically increased upon incubation at 37°C (7.3 ± 1.1, *p* < 0.1 times over 0°C), while the increase in total sAPPβ did not reach statistical significance (Fig. 7A, B). To further confirm that *pal*-sAPPβ was indeed generated by BACE1 cleavage, we performed the assay in presence of increasing concentrations of the BACE inhibitor BACEi IV. The inhibitor prevented the increase in *pal*-sAPPβ levels in a dose-dependent manner (Fig. 7A, B), confirming BACE1-dependent processing of *palAPP*. Although the experiments were performed at a low pH (pH 4) to specifically test BACE1 activity, we probed

for the release of sAPPα in the assay. We detected residual sAPPα in the reaction mixture, but the levels of sAPPα remained unchanged upon incubation at 37°C, confirming that our *in vitro* assay at pH 4 indeed released *pal*-sAPPβ and sAPPβ, but not sAPPα. BACEi IV also had no effect on sAPPα levels, as expected. Similarly to BACEi IV, 1 μM BACE inhibitor dr9 also decreased *pal*-sAPPβ levels in a cell-free *in vitro* BACE-activity assay performed at 37°C (data not shown). The large (~7.3 times over control) increase of *pal*-sAPPβ release at 37°C, not mirrored by total sAPPβ, indicates that *palAPP* is cleaved more efficiently by BACE than non-*palAPP* in our *in vitro* BACE-activity assay in lipid rafts.

Finally, we performed BACE-activity assays on lipid rafts isolated from mouse brains (Fig. 7C). Similarly to cells, we observed increased *pal*-sAPPβ upon BACE activation, which was reduced by BACEi IV in a dose-dependent manner (Fig. 7C). Total sAPPβ levels followed the same trend, although the increase from 0 to 37°C was less pronounced. Together, our data show that lipid raft-bound *palAPP* undergoes BACE1-mediated processing in

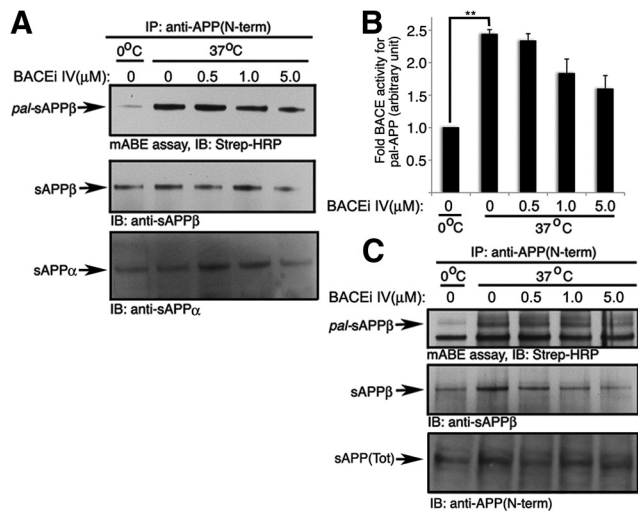


Figure 7. Palmitoylation appears to increase BACE1-mediated cleavage of APP in lipid rafts. **A**, *In vitro* BACE1 cleavage assay shows that *pal*APP in CHO_{APP} cell lipid raft fractions is a good BACE1 substrate. *pal*-sAPP β , sAPP β , and sAPP α are shown. This is a representative figure of three independent experiments. **B**, Quantitation of **A**. Data represent the average of three independent experiments. **C**, *In vitro* BACE cleavage assay on lipid rafts isolated from mouse brains confirms that endogenous brain lipid raft *pal*APP is a good BACE1 substrate, better than total APP in our *in vitro* BACE cleavage assays.

cells and *in vivo*. Together with the DHHC PAT and BACE over-expression/inhibition data above, our results strongly advocate that palmitoylation promotes amyloidogenic processing of APP.

*pal*APP levels are increased with age in the brains of nontransgenic mice

Aging is closely associated with the impaired cognitive performance of AD patients (Buckner, 2004). Here, we asked whether APP palmitoylation is age dependent. To assess the effect of aging on brain *pal*APP levels, we performed ABE assay on cortical extracts from 3-month-old (young) and 18-month-old (older) wild-type nontransgenic mice (Fig. 8A). Eighteen-month-old mice showed a 1.87 ± 0.7 -fold ($p < 0.05$) increase in *pal*APP levels compared to younger mice (Fig. 8B), suggesting a direct correlation between age and increased endogenous APP palmitoylation in mouse brain.

Palmitoylation or ACAT1 inhibitors reduce *pal*APP levels in lipid rafts

To investigate whether *pal*APP levels can be reduced by pharmacological treatments, we used two different palmitoylation inhibitors: 2-bromopalmitate and cerulenin (Figs. 1B, 9A). Both inhibitors decreased palmitoylation of APP in a concentration-dependent manner while also preventing maturation of APP and APP CTF generation (Fig. 9A). Unfortunately, palmitoylation inhibitors are known to be toxic as they severely disturb cellular lipid metabolism (Draper and Smith, 2009).

We and others have found that ACAT1 inhibition reduces A β generation *in vitro*, in cells, and *in vivo* and is a potential therapeutic target to lower A β (Puglielli et al., 2001; Hutter-Paier et al., 2004; Huttunen et al., 2007a, 2010; Bhattacharyya and Kovacs, 2010; Bryleva et al., 2010). Interestingly, the preferred long-chain acyl substrate for ACAT1 is palmitoyl-CoA. Since ACAT inhibition does not affect total APP levels or trafficking of total APP to lipid rafts (see below), we reasoned that it might affect generation of *pal*APP instead. First, we examined palmitoylation of APP in

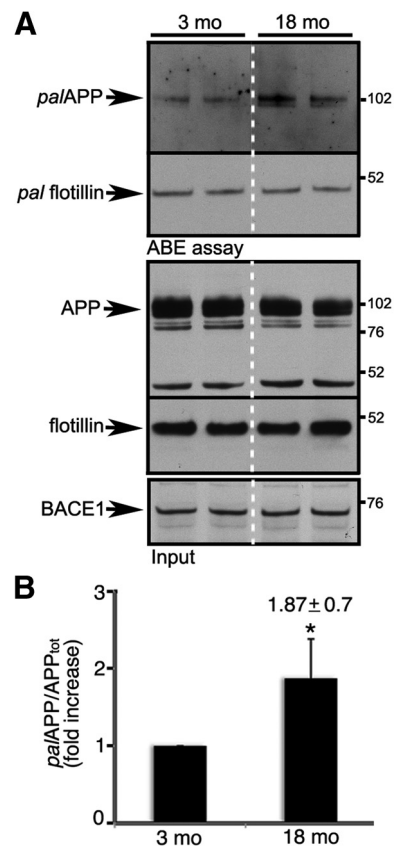


Figure 8. Accumulation of cortical *pal*APP in older nontransgenic mice. **A**, ABE assay of cortical extracts from 3- and 18-month-old mice. *pal*APP levels are higher in 18- versus 3-month-old mice, while *pal*-flotillin levels remain unchanged. Total input of APP, flotillin, and BACE1 were detected with the anti-APP (C66), anti-flotillin, and anti-BACE1 antibodies, respectively. The APP band below 52 kDa is specific. **B**, Quantitation of *pal*APP levels in relation to total APP ($palAPP/APP_{tot}$) from **A**. $*p < 0.05$. $n = 3$ of each age group. Assays were performed in duplicate. Error bars represent the SEM.

AC29_{APP} cells, a genetically mutated CHO cell line that overproduces cholesterol while lacks ACAT1 activity (Puglielli et al., 2001). We have shown previously that this cell line is almost fully unable to produce APP CTFs and A β (Puglielli et al., 2001) (Fig. 9B, left). Glycosylation and trafficking of APP in these cells were largely unaffected by lack of ACAT activity (data not shown). To our surprise, AC29_{APP} cells produced little or no *pal*APP (Fig. 9B, left). Most interestingly, reduction in *pal*APP was also observed in cells treated with the well-known ACAT1 inhibitor CP-113,818 (10 μ M; Fig. 9B, right). We have shown previously that CP-113,818 effectively reduces A β generation *in vivo* and *in vitro* (Hutter-Paier et al., 2004).

Next, we treated CHO_{APP} cells with another well-established ACAT1 inhibitor, CI-1011 or avasimibe. CI-1011 was originally produced by Pfizer and previously reached phase III clinical trials for cardiovascular disease (Tardif et al., 2004). We reported previously that CI-1011 reduces APP CTF levels and A β generation in cells and *in vivo* (Huttunen et al., 2010). Four days of treatment with 5 or 10 μ M CI-1011 severely reduced β - and α -CTF levels, as expected (Fig. 9C). Similarly to CP-113,818, 10 μ M CI-1011 also reduced total *pal*APP level by $\sim 57\%$ (Fig. 9C,D).

To test the effect of ACAT1 inhibition on lipid raft-bound *pal*APP, we first performed lipid raft fractionation on CHO_{APP} cells in absence or presence of 10 μ M CI-1011. Distribution of total APP to lipid raft and nonraft fractions remained largely

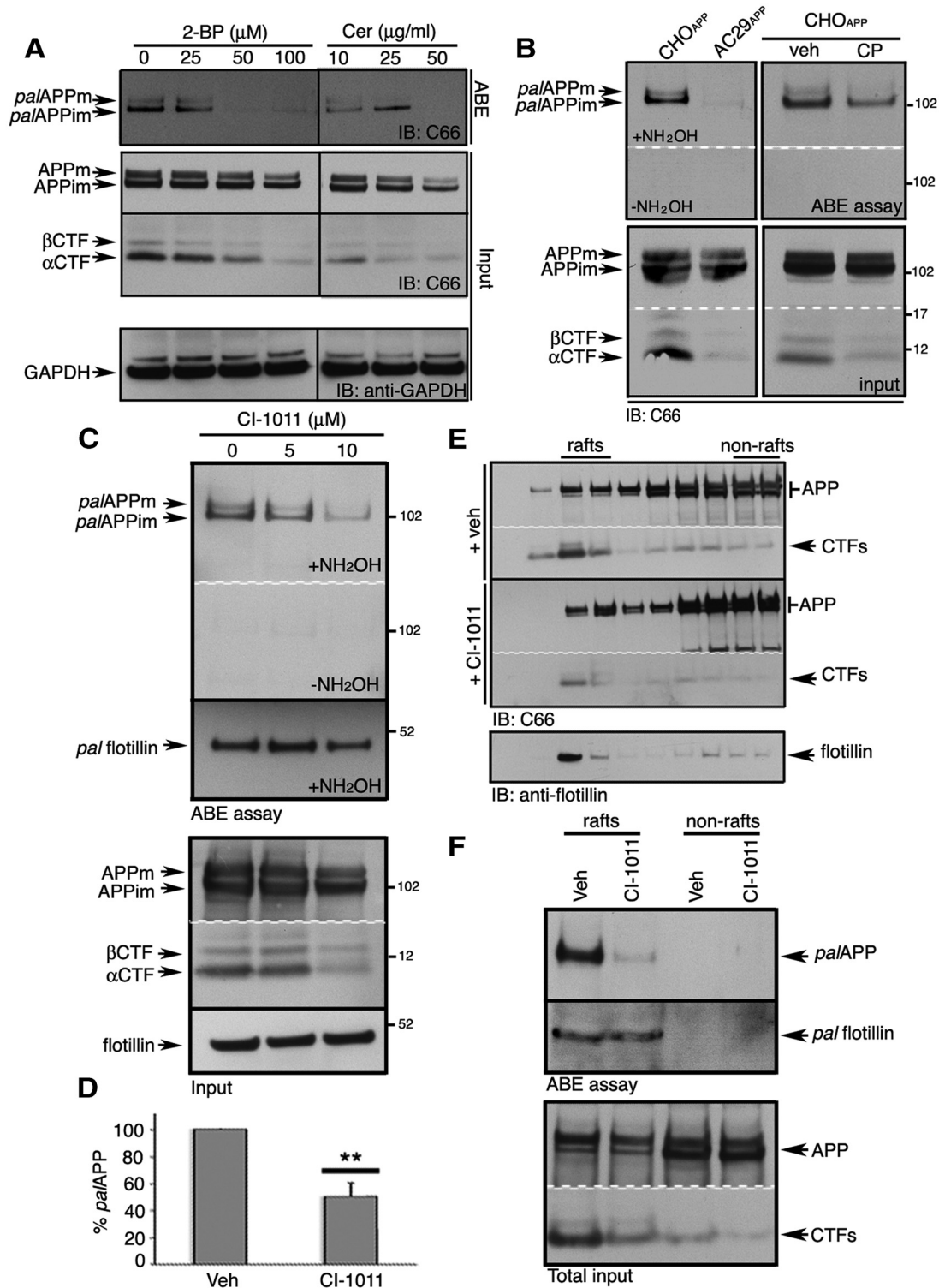


Figure 9. Palmitoylation inhibitors or ACAT inhibitors reduce APP palmitoylation and APP processing. **A**, ABE assay of CHO_{APP} cells after treatment with the indicated amounts of palmitoylation inhibitors, 2-BP or cerulenin (Cer). Both inhibitors reduced *palAPP* and APP CTF levels at concentrations of 50 μM or more. **B**, ACAT inhibition decreases APP palmitoylation. ABE assay showing severe reduction in *palAPP* levels in ACAT-inactive AC29_{APP} cells compared to CHO_{APP} cells. Similarly, treatment of CHO_{APP} cells with 10 μM ACAT inhibitor CP-113,818 (CP) reduced full-length *palAPP* compared to control (veh; ABE assay). Levels of α - and β -CTFs were significantly reduced in AC29_{APP} cells and CP-treated cells (input). **C**, Concentration-dependent reduction in *palAPP* levels by increasing concentrations of the ACAT inhibitor CI-1011 (ABE assay in CHO_{APP} cells). CI-1011 (10 μM) also reduced β - and α -CTF production (input). Levels of *pal* flotillin are also shown. **D**, Quantitation of **C**. CI-1011 (10 μM) induces an ~57% reduction in *palAPP* levels. ** $p < 0.05$. $n = 3$ for each set of experiment. Error bars represent the SEM. **E**, Lipid rafts fractionation of Lubrol extracts of CHO_{APP} cells treated with DMSO vehicle (+ veh) or 10 μM CI-1011 (+ CI-1011) for 4 d showed no significant alteration in APP distribution in raft versus nonraft fractions. **F**, CI-1011-treated cells showed significant reduction in raft-associated *palAPP*. Rafts and nonrafts from untreated (Veh) or CI-1011-treated cells were collected and subjected to ABE analysis to detect *palAPP* or *pal*-flotillin.

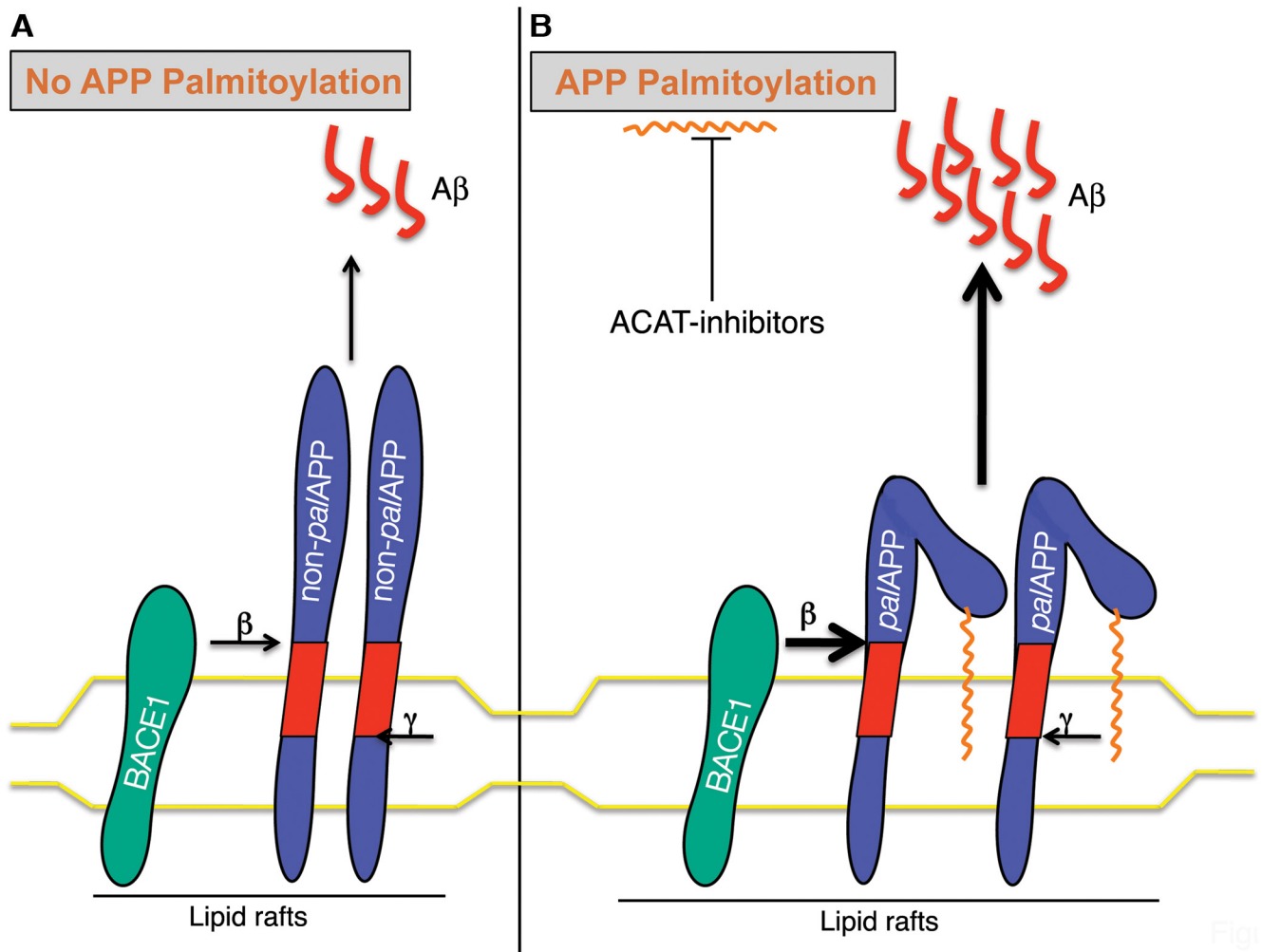


Figure 10. Schematic representation of APP palmitoylation modulating APP processing and A β generation in lipid rafts. **A**, No APP palmitoylation. BACE1 (green) in lipid rafts cleaves APP at the β -cleavage site. Subsequent γ -secretase mediated cleavage (γ) generates A β (red). **B**, APP palmitoylation. APP is palmitoylated, shown as the palmitic moiety (orange) attached to APP (*palAPP*), and recruited to lipid rafts. Our data suggest that palmitoylation may enhance BACE1-mediated cleavage of APP (bold arrow). The final effect is an increased generation of A β . ACAT inhibition attenuates APP palmitoylation, and in turn reduces A β generation.

unaltered upon treatment with CI-1011 (Fig. 9E). Equal amounts of raft and nonraft fractions were isolated from the cells and subjected to ABE assay. As expected, *palAPP* was highly enriched in lipid raft fractions of the untreated cells (Fig. 9F). Importantly, lipid raft-bound *palAPP* levels were reduced by $76.15 \pm 8.9\%$ in cells pretreated with CI-1011 (Fig. 9F). These experiments show that ACAT1 inhibition reduces *palAPP* levels in lipid rafts, likely resulting in the observed decrease in amyloidogenic processing of APP.

Discussion

Our study shows for the first time that APP undergoes palmitoylation. We have identified the palmitoylation sites in the N-terminal E1 luminal domain of APP, at Cys¹⁸⁶ and/or Cys¹⁸⁷. Cys¹⁸⁶ and/or Cys¹⁸⁷ mutants are retained in the ER. Palmitoylation targets APP to lipid rafts, where *palAPP* serves as a good BACE1 substrate. Palmitoylation or ACAT inhibitors severely impair the processing of *palAPP* by α - and β -secretases, presumably due to ER retention and degradation of APP. Together, our data indicate that palmitoylation preferentially targets APP to lipid rafts where *palAPP* serves as a good substrate for BACE1 cleavage and A β generation (Fig. 10).

Protein palmitoylation is a reversible process requiring palmitoylating enzymes (PATs), depalmitoylating enzymes (protein palmitoyl thioesterases), and access to palmitoyl-CoA. At least 24 PATs containing a common ~ 50 aa cysteine-rich domain with a conserved DHHC motif have been shown to catalyze cytoplasmic S-palmitoylation in mammals (Ohno et al., 2006). However, palmitoylation of APP necessarily occurs in the lumen of the secretory pathway since APP's cytoplasmic tail lacks cysteines. Examples of luminal palmitoylation by membrane-bound O-acyltransferases (MBOAT) are becoming increasingly available (Buglino and Resh, 2008). In mammals, secreted proteins such as the morphogens Hedgehog and Wnt, the EGF-receptor ligand Spitz, as well as the peptide hormone ghrelin are post-translationally modified with fatty acids by MBOAT PATs such as Hhat and Porc (Miura and Treisman, 2006; Miura et al., 2006; Buglino and Resh, 2008; Yang et al., 2008). Modification of these secreted proteins occurs in the lumen of the secretory pathway. In addition to MBOAT PATs, the multiple transmembrane domain DHHC PATs could also catalyze luminal palmitoylation if their active sites occasionally faced the lumen. Indeed, several transmembrane proteins such as aquaporin-1 reorient one or more of their transmembrane domains

post-translationally (Lu et al., 2000). APP-interacting DHHC protein (AID)/DHHC-12 was previously reported to interact with APP and suppress APP processing (Mizumaru et al., 2009). However, DHHC-12 does not appear to palmitoylate APP in our experiments (data not shown). To our knowledge, APP is the first transmembrane protein that undergoes S-palmitoylation in the lumen. Identification of APP's palmitoylating enzyme(s) will further clarify the mechanism of luminal palmitoylation of transmembrane proteins and may open up a novel pathway to reduce A β generation.

Luminal palmitoylation of APP also requires transport of highly hydrophobic long-chain palmitoyl-CoA into the lumen (Gooding et al., 2004). Indeed, a brain-specific carnitine palmitoyltransferase 1c has been reported previously to localize in the ER membrane to ensure the entry of palmitoyl-CoA into the ER lumen (Sierra et al., 2008). Alternatively, free palmitic acid may be transported into the ER lumen before being converted to palmitoyl-CoA by luminal acyltransferases (Rys-Sikora and Gill, 1998). Palmitoyl-CoA hydrolase activity was detected in the ER lumen, further confirming that protein palmitoylation and depalmitoylation are not confined to the cytoplasm (Mentlein et al., 1988).

We have identified Cys¹⁸⁶ and Cys¹⁸⁷ as palmitoylated Cys residues in the E1 domain of APP. We have also found that these cysteines strongly regulate trafficking of APP out of the ER. These same cysteines were predicted previously to form disulfide bonds with Cys¹³³ and Cys¹⁵⁸ to stabilize the copper-binding domain of APP. Our data show that lack of disulfide bond formation in Cys¹³³ and Cys¹⁵⁸ mutants may promote palmitoylation at Cys¹⁸⁶ and Cys¹⁸⁷, suggesting that disulfide bond formation at Cys¹⁸⁶ and Cys¹⁸⁷ in APP may regulate its palmitoylation (Fig. 2J). Conversely, Wnt-3a palmitoylation is predicted to regulate disulfide bond formation (Coudreuse and Korswagen, 2007). Interestingly, reduced forms of Cys¹⁸⁶ and Cys¹⁸⁷ appear to promote zinc binding to APP (Bush et al., 1993). This form would also allow the same cysteines to incorporate palmitate via a thioester bond. The precise relationship between palmitoylation, copper/zinc binding, and disulfide bond formation remains to be established for APP's Cys¹⁸⁶ and Cys¹⁸⁷. Our results are consistent with the idea that proper conformation of the E1 domain in APP is important for ER exit and intracellular trafficking of the protein. Disulfide bridges or protein palmitoylation at Cys¹⁸⁶ and/or Cys¹⁸⁷ facilitate this conformation.

palAPP being enriched in lipid rafts is in line with the importance of lipid rafts in APP processing. Palmitoylation often targets proteins to lipid rafts (Cheng et al., 2009; Vetrivel et al., 2009; for review, see Levental et al., 2010). APP, BACE1, and γ -secretase components are all found in detergent-resistant lipid rafts (Vetrivel et al., 2004; 2005; Hattori et al., 2006). Amyloidogenic processing of APP partially depends on lipid rafts whereas nonamyloidogenic α -cleavage of APP occurs mainly in the phospholipid-rich domain of the plasma membrane (Ehehalt et al., 2003). Both monomeric and dimeric species of A β are concentrated in lipid rafts in Tg2576 mice and human AD brains (Lee et al., 1998; Kawarabayashi et al., 2004). Palmitoylation also targets BACE1 and two components of γ -secretase, Aph-1 and Nct, to lipid rafts (Cheng et al., 2009; Vetrivel et al., 2009). Double-transgenic mice expressing APP and palmitoylation-deficient Aph-1 or Nct show reduced A β deposition (Meckler et al., 2010). Interestingly, artificial targeting of BACE to the lipid rafts enhanced β -cleavage of APP (Cordy et al., 2003). Our data indicate, but do not confirm, enhanced β -secretase-mediated processing of *palAPP* in lipid rafts. Surprisingly, wild-type APP is considered a poor substrate for BACE1 (Stockley and O'Neill, 2008). Strict biochemical quantitation of BACE1-mediated cleavage of

palAPP will be required to determine whether palmitoylation does enhance APP processing in lipid rafts. An additional question is whether *palAPP* outside lipid rafts serves as a good BACE1 substrate. The main pool of APP resides outside the lipid rafts, but the relative concentration of *palAPP* in these fractions was too low for our *in vitro* BACE cleavage assays. Nevertheless, *palAPP* is also found outside of lipid rafts, where it may regulate APP processing.

Cortical extracts from nontransgenic mice showed an age-dependent increase in *palAPP* levels (Fig. 8). It is well known that both AD and aging are characterized by elevated A β accumulation, at a much higher degree in the brains of patients affected by AD than during normal aging (Price et al., 1992; Haass and Selkoe, 2007; Reddy and Beal, 2008). An age-dependent increase in BACE1 activity and levels may lead to a rise in A β generation in some, but not all, AD patients (Fukumoto et al., 2002, 2004). It remains to be investigated whether *palAPP* levels are increased in human aging and AD brains. Elevated *palAPP*, perhaps leading to more A β generation, may contribute to widespread A β accumulation in these brains.

Treatment with the palmitoylation inhibitors cerulenin and 2-bromopalmitate not only prevented APP palmitoylation, but also resulted in severe loss of its processing and maturation, suggesting that palmitoylation plays an important role in APP metabolism. In recent years, the key role of palmitoylation has become increasingly clear in multiple diseases such as Huntington's disease, various cardiovascular and T-cell mediated immune disorders, as well as cancer (Draper and Smith, 2009). To date, two types of palmitoylation inhibitors have been identified, lipid-based palmitoylation inhibitors such as 2-BP or cerulenin, and non-lipid palmitoylation inhibitors such as the chemotypes Compounds I, II, III, and IV (Ducker et al., 2006). Lipid-based inhibitors broadly inhibit the palmitoylation of proteins and affect fatty acid biosynthesis. In contrast, non-lipid palmitoylation inhibitors have been shown to selectively inhibit the palmitoylation of different PAT recognition motifs (Ducker et al., 2006; Draper and Smith, 2009). However, no small-molecule PAT inhibitor has yet been developed for therapeutic purposes.

ACAT inhibitors reduced *palAPP* levels in lipid rafts, and lack of ACAT activity in AC29 cells prevented palmitoylation of APP. One possible explanation for how ACAT inhibitors reduce *palAPP* is that ACAT inhibition slightly increases ER free cholesterol (Huttunen et al., 2009), which then may limit availability of palmitic acid and/or palmitoyl-CoA inside the ER lumen. Alternatively, slightly increased free cholesterol levels may indirectly impact lipid raft levels enriched with proteases for the amyloidogenic pathway. Cholesterol binds directly to the transmembrane domain of APP (Bodovitz and Klein, 1996; Kojro et al., 2001; Barrett et al., 2012). Cholesterol has also been reported previously to directly interact with the palmitoyl moiety of the μ -opioid receptor (OPRM1) and thus regulate receptor function (Zheng et al., 2012). Simvastatin treatment reduced OPRM1 signaling (Zheng et al., 2012). Thus, changes in cellular cholesterol induced by ACAT inhibition or other CNS-relevant lipids such as 24-hydroxycholesterol could regulate *palAPP* levels and/or function. More research will be needed to explore this event at a mechanistic level. Numerous ACAT inhibitors have already been developed against atherosclerosis and hypercholesterolemia and tested in clinical trials (Farese, 2006). However, ACAT inhibitors are currently not marketed. Our previous studies confirmed by others clearly support ACAT inhibition as a strategy for regulating amyloid pathology in the brain (Puglielli et al., 2001; Hutter-Paier et al., 2004; Huttunen et al., 2010). Collectively, our previ-

ous studies and the current mechanistic finding that ACAT inhibitors reduce palmitoylation of APP warrant further development of ACAT inhibitors as a therapeutic strategy for AD.

References

- Barnham KJ, McKinstry WJ, Multhaup G, Galatis D, Morton CJ, Curtain CC, Williamson NA, White AR, Hinds MG, Norton RS, Beyreuther K, Masters CL, Parker MW, Cappai R (2003) Structure of the Alzheimer's disease amyloid precursor protein copper binding domain. A regulator of neuronal copper homeostasis. *J Biol Chem* 278:17401–17407. [CrossRef Medline](#)
- Barrett PJ, Song Y, Van Horn WD, Hustedt EJ, Schafer JM, Hadziselimovic A, Beel AJ, Sanders CR (2012) The amyloid precursor protein has a flexible transmembrane domain and binds cholesterol. *Science* 336:1168–1171. [CrossRef Medline](#)
- Bhattacharyya R, Kovacs DM (2010) ACAT inhibition and amyloid beta reduction. *Biochim Biophys Acta* 1801:960–965. [CrossRef Medline](#)
- Bhattacharyya R, Wedegaertner PB (2000) G alpha 13 requires palmitoylation for plasma membrane localization, Rho-dependent signaling, and promotion of p115RhoGEF membrane binding. *J Biol Chem* 275:14992–14999. [CrossRef Medline](#)
- Bodovitz S, Klein WL (1996) Cholesterol modulates alpha-secretase cleavage of amyloid precursor protein. *J Biol Chem* 271:4436–4440. [CrossRef Medline](#)
- Brown DA (2006) Lipid rafts, detergent-resistant membranes, and raft targeting signals. *Physiology (Bethesda)* 21:430–439. [CrossRef](#)
- Bryleva EY, Rogers MA, Chang CC, Buen F, Harris BT, Rousselet E, Seidah NG, Oddo S, LaFerla FM, Spencer SA, Hickey WF, Chang TY (2010) ACAT1 gene ablation increases 24(S)-hydroxycholesterol content in the brain and ameliorates amyloid pathology in mice with AD. *Proc Natl Acad Sci U S A* 107:3081–3086. [CrossRef Medline](#)
- Buckner RL (2004) Memory and executive function in aging and AD: multiple factors that cause decline and reserve factors that compensate. *Neuron* 44:195–208. [CrossRef Medline](#)
- Buglino JA, Resh MD (2008) Hhat is a palmitoyltransferase with specificity for N-palmitoylation of Sonic Hedgehog. *J Biol Chem* 283:22076–22088. [CrossRef Medline](#)
- Bush AI, Multhaup G, Moir RD, Williamson TG, Small DH, Rumble B, Pollwein P, Beyreuther K, Masters CL (1993) A novel zinc(II) binding site modulates the function of the A4 amyloid protein precursor of Alzheimer's disease. *J Biol Chem* 268:16109–16112. [Medline](#)
- Charollais J, Van Der Goot FG (2009) Palmitoylation of membrane proteins (Review). *Mol Membr Biol* 26:55–66. [CrossRef Medline](#)
- Charron G, Zhang MM, Yount JS, Wilson J, Raghavan AS, Shamir E, Hang HC (2009) Robust fluorescent detection of protein fatty-acylation with chemical reporters. *J Am Chem Soc* 131:4967–4975. [CrossRef Medline](#)
- Cheng H, Vetrivel KS, Drisdell RC, Meckler X, Gong P, Leem JY, Li T, Carter M, Chen Y, Nguyen P, Iwatsubo T, Tomita T, Wong PC, Green WN, Kounnas MZ, Thinakaran G (2009) S-palmitoylation of gamma-secretase subunits nicastrin and APH-1. *J Biol Chem* 284:1373–1384. [Medline](#)
- Cordy JM, Hussain I, Dingwall C, Hooper NM, Turner AJ (2003) Exclusively targeting beta-secretase to lipid rafts by GPI-anchor addition up-regulates beta-site processing of the amyloid precursor protein. *Proc Natl Acad Sci U S A* 100:11735–11740. [CrossRef Medline](#)
- Coudreuse D, Korswagen HC (2007) The making of Wnt: new insights into Wnt maturation, sorting and secretion. *Development* 134:3–12. [CrossRef Medline](#)
- De Strooper B, Annaert W (2000) Proteolytic processing and cell biological functions of the amyloid precursor protein. *J Cell Sci* 113:1857–1870. [Medline](#)
- Draper JM, Smith CD (2009) Palmitoyl acyltransferase assays and inhibitors (Review). *Mol Membr Biol* 26:5–13. [CrossRef Medline](#)
- Ducker CE, Griffel LK, Smith RA, Keller SN, Zhuang Y, Xia Z, Diller JD, Smith CD (2006) Discovery and characterization of inhibitors of human palmitoyl acyltransferases. *Mol Cancer Ther* 5:1647–1659. [CrossRef Medline](#)
- Ehehalt R, Keller P, Haass C, Thiele C, Simons K (2003) Amyloidogenic processing of the Alzheimer beta-amyloid precursor protein depends on lipid rafts. *J Cell Biol* 160:113–123. [CrossRef Medline](#)
- Farese RV Jr (2006) The nine lives of ACAT inhibitors. *Arterioscler Thromb Vasc Biol* 26:1684–1686. [CrossRef Medline](#)
- Fukata M, Fukata Y, Adesnik H, Nicoll RA, Brecht DS (2004) Identification of PSD-95 palmitoylating enzymes. *Neuron* 44:987–996. [CrossRef Medline](#)
- Fukata Y, Fukata M (2010) Protein palmitoylation in neuronal development and synaptic plasticity. *Nat Rev Neurosci* 11:161–175. [CrossRef Medline](#)
- Fukumoto H, Cheung BS, Hyman BT, Irizarry MC (2002) Beta-secretase protein and activity are increased in the neocortex in Alzheimer disease. *Arch Neurol* 59:1381–1389. [CrossRef Medline](#)
- Fukumoto H, Rosene DL, Moss MB, Raju S, Hyman BT, Irizarry MC (2004) Beta-secretase activity increases with aging in human, monkey, and mouse brain. *Am J Pathol* 164:719–725. [CrossRef Medline](#)
- Gooding JM, Shayeghi M, Saggerson ED (2004) Membrane transport of fatty acylcarnitine and free L-carnitine by rat liver microsomes. *Eur J Biochem* 271:954–961. [CrossRef Medline](#)
- Haass C, Selkoe DJ (2007) Soluble protein oligomers in neurodegeneration: lessons from the Alzheimer's amyloid beta-peptide. *Nat Rev Mol Cell Biol* 8:101–112. [CrossRef Medline](#)
- Haass C, Koo EH, Mellon A, Hung AY, Selkoe DJ (1992) Targeting of cell-surface beta-amyloid precursor protein to lysosomes: alternative processing into amyloid-bearing fragments. *Nature* 357:500–503. [CrossRef Medline](#)
- Haass C, Kaether C, Thinakaran G, Sisodia S (2012) Trafficking and proteolytic processing of APP. *Cold Spring Harb Perspect Med* 2:a006270. [CrossRef Medline](#)
- Hattori C, Asai M, Onishi H, Sasagawa N, Hashimoto Y, Saido TC, Maruyama K, Mizutani S, Ishiura S (2006) BACE1 interacts with lipid raft proteins. *J Neurosci Res* 84:912–917. [CrossRef Medline](#)
- Hutter-Paier B, Huttunen HJ, Puglielli L, Eckman CB, Kim DY, Hofmeister A, Moir RD, Domnitz SB, Frosch MP, Windisch M, Kovacs DM (2004) The ACAT inhibitor CP-113,818 markedly reduces amyloid pathology in a mouse model of Alzheimer's disease. *Neuron* 44:227–238. [CrossRef Medline](#)
- Huttunen HJ, Guénette SY, Peach C, Greco C, Xia W, Kim DY, Barren C, Tanzi RE, Kovacs DM (2007b) HtrA2 regulates beta-amyloid precursor protein (APP) metabolism through endoplasmic reticulum-associated degradation. *J Biol Chem* 282:28285–28295. [CrossRef Medline](#)
- Huttunen HJ, Peach C, Bhattacharyya R, Barren C, Pettingell W, Hutter-Paier B, Windisch M, Berezovska O, Kovacs DM (2009) Inhibition of acyl-coenzyme A: cholesterol acyl transferase modulates amyloid precursor protein trafficking in the early secretory pathway. *Faseb J* 23:3819–3828. [CrossRef Medline](#)
- Huttunen HJ, Havas D, Peach C, Barren C, Duller S, Xia W, Frosch MP, Hutter-Paier B, Windisch M, Kovacs DM (2010) The acyl-coenzyme A: cholesterol acyltransferase inhibitor CI-1011 reverses diffuse brain amyloid pathology in aged amyloid precursor protein transgenic mice. *J Neuropathol Exp Neurol* 69:777–788. [CrossRef Medline](#)
- Huttunen HJ, Greco C, Kovacs DM (2007a) Knockdown of ACAT-1 reduces amyloidogenic processing of APP. *FEBS Lett* 581:1688–1692. [CrossRef Medline](#)
- Iwatsubo T, Odaka A, Suzuki N, Mizusawa H, Nukina N, Ihara Y (1994) Visualization of A beta 42(43) and A beta 40 in senile plaques with end-specific A beta monoclonals: evidence that an initially deposited species is A beta 42(43). *Neuron* 13:45–53. [CrossRef Medline](#)
- Kang R, Wan J, Arstikaitis P, Takahashi H, Huang K, Bailey AO, Thompson JX, Roth AF, Drisdell RC, Mastro R, Green WN, Yates JR 3rd, Davis NG, El-Husseini A (2008) Neural palmitoyl-proteomics reveals dynamic synaptic palmitoylation. *Nature* 456:904–909. [CrossRef Medline](#)
- Kawarabayashi T, Shoji M, Younkin LH, Wen-Lang L, Dickson DW, Murakami T, Matsubara E, Abe K, Ashe KH, Younkin SG (2004) Dimeric amyloid beta protein rapidly accumulates in lipid rafts followed by apolipoprotein E and phosphorylated tau accumulation in the Tg2576 mouse model of Alzheimer's disease. *J Neurosci* 24:3801–3809. [CrossRef Medline](#)
- Kim DY, Carey BW, Wang H, Ingano LA, Binshtok AM, Wertz MH, Pettinelli WH, He P, Lee VM, Woolf CJ, Kovacs DM (2007) BACE1 regulates voltage-gated sodium channels and neuronal activity. *Nat Cell Biol* 9:755–764. [CrossRef Medline](#)
- Kim DY, Gersbacher MT, Inquimbert P, Kovacs DM (2011) Reduced sodium channel Nav1.1 levels in BACE1-null mice. *J Biol Chem* 286:8106–8116. [CrossRef Medline](#)
- Kojro E, Fahrenholz F (2005) The non-amyloidogenic pathway: structure and function of alpha-secretases. *Subcell Biochem* 38:105–127. [CrossRef Medline](#)

- Kojro E, Gimpl G, Lammich S, Marz W, Fahrenholz F (2001) Low cholesterol stimulates the nonamyloidogenic pathway by its effect on the alpha-secretase ADAM 10. *Proc Natl Acad Sci U S A* 98:5815–5820. [CrossRef Medline](#)
- Komekado H, Yamamoto H, Chiba T, Kikuchi A (2007) Glycosylation and palmitoylation of Wnt-3a are coupled to produce an active form of Wnt-3a. *Genes Cells* 12:521–534. [CrossRef Medline](#)
- Lee SJ, Liyanage U, Bickel PE, Xia W, Lansbury PT Jr, Kosik KS (1998) A detergent-insoluble membrane compartment contains A beta *in vivo*. *Nat Med* 4(6):730–734. [CrossRef](#)
- Levental I, Lingwood D, Grzybek M, Coskun U, Simons K (2010) Palmitoylation regulates raft affinity for the majority of integral raft proteins. *Proc Natl Acad Sci U S A* 107:22050–22054. [CrossRef Medline](#)
- Lu Y, Turnbull IR, Bragin A, Carveth K, Verkman AS, Skach WR (2000) Reorientation of aquaporin-1 topology during maturation in the endoplasmic reticulum. *Mol Biol Cell* 11:2973–2985. [Medline](#)
- Meckler X, Roseman J, Das P, Cheng H, Pei S, Keat M, Kassarian B, Golde TE, Parent AT, Thinakaran G (2010) Reduced Alzheimer's disease β -amyloid deposition in transgenic mice expressing S-palmitoylation-deficient APH1aL and nicastrin. *J Neurosci* 30:16160–16169. [CrossRef Medline](#)
- Mentlein R, Rix-Matzen H, Heymann E (1988) Subcellular localization of non-specific carboxylesterases, acylcarnitine hydrolase, monoacylglycerol lipase and palmitoyl-CoA hydrolase in rat liver. *Biochim Biophys Acta* 964:319–328. [CrossRef Medline](#)
- Mitchell DA, Vasudevan A, Linder ME, Deschenes RJ (2006) Protein palmitoylation by a family of DHHC protein S-acyltransferases. *J Lipid Res* 47:1118–1127. [CrossRef Medline](#)
- Miura GI, Treisman JE (2006) Lipid modification of secreted signaling proteins. *Cell Cycle* 5:1184–1188. [CrossRef Medline](#)
- Miura GI, Buglino J, Alvarado D, Lemmon MA, Resh MD, Treisman JE (2006) Palmitoylation of the EGFR ligand Spitz by Rasp increases Spitz activity by restricting its diffusion. *Dev Cell* 10:167–176. [CrossRef Medline](#)
- Mizumaru C, Saito Y, Ishikawa T, Yoshida T, Yamamoto T, Nakaya T, Suzuki T (2009) Suppression of APP-containing vesicle trafficking and production of β -amyloid by AID/DHHC-12 protein. *J Neurochem* 111:1213–1224. [CrossRef Medline](#)
- Ohno Y, Kihara A, Sano T, Igarashi Y (2006) Intracellular localization and tissue-specific distribution of human and yeast DHHC cysteine-rich domain-containing proteins. *Biochim Biophys Acta* 1761:474–483. [CrossRef Medline](#)
- Price DL, Walker LC, Martin LJ, Sisodia SS (1992) Amyloidosis in aging and Alzheimer's disease. *Am J Pathol* 141:767–772. [Medline](#)
- Puglielli L, Konopka G, Pack-Chung E, Ingano LA, Berezovska O, Hyman BT, Chang TY, Tanzi RE, Kovacs DM (2001) Acyl-coenzyme A: cholesterol acyltransferase modulates the generation of the amyloid [beta]-peptide. *Nat Cell Biol* 3:905–912. [CrossRef Medline](#)
- Reddy PH, Beal MF (2008) Amyloid beta, mitochondrial dysfunction and synaptic damage: implications for cognitive decline in aging and Alzheimer's disease. *Trends Mol Med* 14:45–53. [CrossRef Medline](#)
- Resh MD (2004) Membrane targeting of lipid modified signal transduction proteins. *Subcell Biochem* 37:217–232. [CrossRef Medline](#)
- Resh MD (2006) Palmitoylation of ligands, receptors, and intracellular signaling molecules. *Sci STKE* 2006: re14. [CrossRef Medline](#)
- Rocks O, Peyker A, Kahms M, Verveer PJ, Koerner C, Lumbierres M, Kuhlmann J, Waldmann H, Wittinghofer A, Bastiaens PI (2005) An acylation cycle regulates localization and activity of palmitoylated Ras isoforms. *Science* 307:1746–1752. [CrossRef Medline](#)
- Roth AF, Wan J, Bailey AO, Sun B, Kuchar JA, Green WN, Phinney BS, Yates JR 3rd, Davis NG (2006) Global analysis of protein palmitoylation in yeast. *Cell* 125:1003–1013. [CrossRef Medline](#)
- Rys-Sikora KE, Gill DL (1998) Fatty acid-mediated calcium sequestration within intracellular calcium pools. *J Biol Chem* 273:32627–32635. [CrossRef Medline](#)
- Selkoe DJ (1998) The cell biology of beta-amyloid precursor protein and presenilin in Alzheimer's disease. *Trends Cell Biol* 8:447–453. [CrossRef Medline](#)
- Sierra AY, Gratacós E, Carrasco P, Clotet J, Ureña J, Serra D, Asins G, Hegardt FG, Casals N (2008) CPT1c is localized in endoplasmic reticulum of neurons and has carnitine palmitoyltransferase activity. *J Biol Chem* 283:6878–6885. [CrossRef Medline](#)
- Steiner H, Fluhrer R, Haass C (2008) Intramembrane proteolysis by [gamma]-secretase. *J Biol Chem* 283:29627–29631. [CrossRef Medline](#)
- Stockley JH, O'Neill C (2008) Understanding BACE1: essential protease for amyloid-beta production in Alzheimer's disease. *Cell Mol Life Sci* 65:3265–3289. [CrossRef Medline](#)
- Tanzi RE, Moir RD, Wagner SL (2004) Clearance of Alzheimer's Abeta peptide: the many roads to perdition. *Neuron* 43:605–608. [CrossRef Medline](#)
- Tardif JC, Grégoire J, L'Allier PL, Anderson TJ, Bertrand O, Reeves F, Title LM, Alfonso F, Schampaert E, Hassan A, McLain R, Pressler ML, Ibrahim R, Lespérance J, Blue J, Heinenon T, Rodés-Cabau J (2004) Effects of the acyl coenzyme A:cholesterol acyltransferase inhibitor avasimibe on human atherosclerotic lesions. *Circulation* 110:3372–3377. [CrossRef Medline](#)
- Thinakaran G, Koo EH (2008) Amyloid precursor protein trafficking, processing, and function. *J Biol Chem* 283:29615–29619. [CrossRef Medline](#)
- Vetrivel KS, Cheng H, Lin W, Sakurai T, Li T, Nukina N, Wong PC, Xu H, Thinakaran G (2004) Association of gamma-secretase with lipid rafts in post-Golgi and endosome membranes. *J Biol Chem* 279:44945–44954. [CrossRef Medline](#)
- Vetrivel KS, Cheng H, Kim SH, Chen Y, Barnes NY, Parent AT, Sisodia SS, Thinakaran G (2005) Spatial segregation of gamma-secretase and substrates in distinct membrane domains. *J Biol Chem* 280:25892–25900. [CrossRef Medline](#)
- Vetrivel KS, Meckler X, Chen Y, Nguyen PD, Seidah NG, Vassar R, Wong PC, Fukata M, Kounnas MZ, Thinakaran G (2009) Alzheimer disease Abeta production in the absence of S-palmitoylation-dependent targeting of BACE1 to lipid rafts. *J Biol Chem* 284:3793–3803. [Medline](#)
- Wada S, Morishima-Kawashima M, Qi Y, Misono H, Shimada Y, Ohno-Iwashita Y, Ihara Y (2003) Gamma-secretase activity is present in rafts but is not cholesterol-dependent. *Biochemistry* 42:13977–13986. [CrossRef Medline](#)
- Walsh DM, Selkoe DJ (2004) Deciphering the molecular basis of memory failure in Alzheimer's disease. *Neuron* 44:181–193. [CrossRef Medline](#)
- Wan J, Roth AF, Bailey AO, Davis NG (2007) Palmitoylated proteins: purification and identification. *Nat Protoc* 2:1573–1584. [CrossRef Medline](#)
- Yamakawa H, Yagishita S, Futai E, Ishiura S (2010) beta-Secretase inhibitor potency is decreased by aberrant beta-cleavage location of the “Swedish mutant” amyloid precursor protein. *J Biol Chem* 285:1634–1642. [CrossRef Medline](#)
- Yang J, Brown MS, Liang G, Grishin NV, Goldstein JL (2008) Identification of the acyltransferase that octanoylates ghrelin, an appetite-stimulating peptide hormone. *Cell* 132:387–396. [CrossRef Medline](#)
- Yang W, Di Vizio D, Kirchner M, Steen H, Freeman MR (2010) Proteome scale characterization of human S-acylated proteins in lipid raft-enriched and non-raft membranes. *Mol Cell Proteomics* 9:54–70. [CrossRef Medline](#)
- Zheng H, Pearsall EA, Hurst DP, Zhang Y, Chu J, Zhou Y, Reggio PH, Loh HH, Law PY (2012) Palmitoylation and membrane cholesterol stabilize mu-opioid receptor homodimerization and G protein coupling. *BMC Cell Biol* 13:6. [CrossRef Medline](#)
- Zhou F, Xue Y, Yao X, Xu Y (2006) CSS-Palm: palmitoylation site prediction with a clustering and scoring strategy (CSS). *Bioinformatics* 22:894–896. [CrossRef Medline](#)